

Impact of Transmission Dynamics and Treatment Uptake, Frequency and Timing on the Cost-effectiveness of Directly Acting Antivirals for Hepatitis C Virus Infection

Soham Das^a, Ajit Sood^b, Vandana Midha^c, Arshdeep Singh^b, Pranjl Sharma^d, Varun Ramamohan^a

^a*Department of Mechanical Engineering, Indian Institute of Technology Delhi, Hauz Khas, New Delhi, 110016, Delhi, India*

^b*Department of Gastroenterology, Dayanand Medical College and Hospital, Ludhiana, 141001, Punjab, India*

^c*Department of Medicine, Dayanand Medical College and Hospital, Ludhiana, 141001, Punjab, India*

^d*Department of Community Medicine, Dayanand Medical College and Hospital, Ludhiana, 141001, Punjab, India*

Abstract

Cost-effectiveness analyses, based on decision-analytic models of disease progression and treatment, are routinely used to assess the economic value of a new intervention and consequently inform reimbursement decisions for the intervention. Many decision-analytic models developed to assess the economic value of highly effective directly acting antiviral (DAA) treatments for the hepatitis C virus (HCV) infection do not incorporate the transmission dynamics of HCV, accounting for which is required to estimate the number of downstream infections prevented by curing an infection. In this study, we develop and validate a comprehensive agent-based simulation (ABS) model of HCV transmission dynamics in the Indian context and use it to: (a) quantify the extent to which the cost-effectiveness of a DAA is underestimated - as a function of its uptake rate - if disease transmission dynamics are not considered in a cost-effectiveness analysis model; and (b) quantify the impact of the frequency and timing of treatment within a disease surveillance period, also as a function of uptake rate, on DAA cost-effectiveness. The process of accomplishing the above research objectives also motivated the development of a novel random sampling and allocation approach, along with associated theoretical grounding, to estimate individual-level outcomes within an ABS that incurs substantially lower computational expense than the benchmark incremental accumulation approach.

Keywords: OR in developing countries, Hepatitis C virus, Agent-based simulation, Transmission dynamics, Treatment frequency and timing

*Corresponding Author

Email address: varunr@mech.iitd.ac.in (Varun Ramamohan)

1. Introduction

The hepatitis C virus (HCV) infection is the leading cause of liver cirrhosis and hepatocellular carcinoma (HCC), and globally affects as many as 58 million people (WHO, 2024). The global prevalence of HCV is approximately 1% (CDC, 2024); however, it is much higher in many developing countries. For example, it is 11.6% in Pakistan, 5.9% in Gabon in Africa, and 3.0% in Uzbekistan (CDC, 2024). In India, where our study is situated, the prevalence of HCV was estimated at 0.5%-1.5% (Sood et al., 2018). However, there is considerable variation in the prevalence of HCV within India, with certain states (provinces) such as Punjab reporting a prevalence as high as 3.6% (Sood et al., 2018). In such regions, poor access to screening and treatment has been identified as a key contributor to mortality from the disease (WHO, 2024). Thus a comprehensive effort to improve HCV outcomes in these regions would involve accurately characterizing the cost-effectiveness of HCV treatment, and then quantifying the health and economic impact of the timing and frequency of HCV screening and treatment programs so that their cost-effectiveness can be optimized. In this study, we accomplish this via an agent-based simulation of HCV transmission dynamics situated in the Indian state of Punjab.

Cost-effectiveness analyses are routinely used across the world for comparing interventions for health conditions, and in particular, for informing reimbursement decisions for new interventions (such as a new drug or a new disease screening policy) made by payers such as public health agencies (e.g., the United Kingdom) or insurance companies (e.g., in the United States). Such analyses quantify the health and cost value of an intervention - typically in terms of quality-adjusted life years (QALYs) and costs - via the use of decision-analytic models such as Markov chains, decision trees, discrete-event or agent-based simulations (Chhatwal et al., 2016). In the context of HCV, such analyses have been used to, for example, determine optimal policies for prioritizing HCV treatment in US prisons (Ayer et al., 2019), and to quantify and summarize the health and cost benefits of universal screening and treatment with next-generation directly acting antiviral (DAA) drug regimens in India (Chugh et al., 2021). Models employed in cost-effectiveness analyses of interventions for infectious diseases ideally must consider transmissions of infections, so that the population-level health and cost benefits of *preventing* new infections, in addition to those of *curing* existing infections, are also considered when making the reimbursement decision. However, as documented in literature reviews of cost-effectiveness analyses conducted for HCV (Chhatwal et al., 2016) and HIV/AIDS (Gopalappa et al., 2017), very few such models incorporate disease transmission. This is the case for cost-effectiveness analyses conducted in the

Indian context as well. In fact, in our knowledge, a comprehensive model of HCV transmission dynamics that considers the inherent stochasticity of infectious disease transmission has not yet been developed for the Indian - and indeed for the developing world - contexts.

The extent to which HCV treatment prevents new infections, and indeed is cost-effective, depends on its uptake rate - that is, the proportion of those infected who complete the treatment regimen. However, the marginal costs of expanding treatment to more infected patients may increase substantially beyond a certain threshold uptake rate. Therefore, given the above context, the following research questions arise: (a) quantitatively, what is the impact of *not* incorporating transmissions on the cost-effectiveness of treatment; (b) what is the impact of uptake rate on the cost-effectiveness of treatment, and on the underestimation of health and cost benefits when transmissions are not considered; and (c) how can we determine the threshold uptake rate beyond which expanding reimbursable access to treatment is no longer cost-effective? We address these research questions as part of our first research objective (*RO1*): *quantify the impact of incorporating HCV transmission dynamics on the epidemiological, health and cost outcomes associated with HCV treatment as a function of its uptake rate.*

HCV is a disease with slow progression, with patients typically spending long durations in the initial fibrotic stages before progressing to the cirrhotic stages or developing hepatocellular carcinoma. This implies that under resource-constrained conditions that characterize many developing countries, the timing and frequency of screening and treatment programmes for HCV may not necessarily need to be similar to that of other diseases (even HIV). For example, annual frequencies may not be cost-effective in terms of both health and economic outcomes. Further, the timing of deployment of interventions may also need careful consideration. For instance, consider a disease surveillance programme initiated at T_0 and slated to run until T_N . If resource constraints allow organizing one screening and treatment camp during the surveillance programme, then the question arises as to whether running the camp at T_0 would be more beneficial in terms of health and cost outcomes than at T_N , given the slow progression and (relatively) slow spread of the disease. Similarly, resources permitting, would running three camps be more cost-effective than two? If not, for the two-camp policy, when should they be held during the surveillance period? We address these questions as part of our second research objective (*RO2*): *quantitatively characterize the impact of timing and frequency of HCV treatment, as a function of its uptake rate, with respect to a disease surveillance period.*

We accomplish the above research objectives by developing an agent-based simulation model

(ABM) of HCV transmission dynamics in the Indian state of Punjab, which has one of the highest HCV prevalences in the country (Sood et al., 2018). ABMs are a natural choice here (Ghaderi, 2022; Duma & Aringhieri, 2023; Nguyen et al., 2024) given their capability of incorporating the individual-based heterogeneity and stochasticity inherent to infectious disease transmission dynamics, and have previously been used to evaluate HCV treatment policy in the developed world (Ayer et al., 2019). Using ABMs to evaluate the cost-effectiveness of interventions for diseases such as HCV requires simulating the progression of disease for each infected agent over their lifetime - in other words, *lifetime horizon* outcomes need to be estimated. This involves considerable computational expense given that (a) life expectancies are not affected substantially for most HCV patients (quality of life, however, is); (b) day-long time steps were found to be appropriate for advancing the ABM; (c) the run length of a single replication was 60 simulation years; and (d) a relatively large number of agents were considered in our ABM. Such computational expense can arise in ABMs of any infectious disease with natural histories significantly longer than the ABM or intervention evaluation time horizon; for instance, in ABMs developed to model HIV transmission or even tuberculosis (TB). This motivated our third (methodological) research objective (*RO3*): *develop, with mathematical grounding, a computationally efficient method for estimating lifetime horizon outcomes, preserving their inherent stochasticity, for ABMs of infectious disease transmission dynamics.*

In our knowledge, these questions have not previously been addressed in the extant literature. The answers to these questions may find application beyond just HCV: for example, they have not in our knowledge also been addressed for HIV or TB via a comprehensive modeling study such as ours - in particular, not in the developing world.

The remainder of the paper is organized as follows. In Section 2, we discuss the relevant literature and describe our research contributions. In Section 3, we describe the ABM development and our proposed method to reduce its computational expense (i.e., *RO3*). In Section 4, we discuss computational experiments conducted to address *RO1* and *RO2*, and we conclude in Section 5 with a discussion of the potential impact of our study and avenues for future research.

2. Literature Review

In this section, we discuss the literature relevant to research objectives *RO1* through *RO3*, and discuss our research contributions with respect to each objective. Prior to this, we provide a brief overview of the different types of models that have been developed for assessing the epidemiological, health and economic impact of HCV treatment and/or screening, with a focus on treatment

with DAAs. Further, in Table 1 below, we describe the type of transmission model, transmission modes considered, type of disease progression model, the geography of analysis, whether single or multiple treatment uptake rates and frequencies were considered, whether timing of treatment was considered, the outcomes estimation approach, and the types of outcomes generated by the model. In other words, this table summarizes the literature relevant to all three research objectives.

HCV treatment and/or screening impact assessment models are either static or dynamic models. Static models assume that the force of infection associated with HCV is constant throughout the period of evaluation, whereas dynamic models assume that the force of infection at each point in time depends upon the number infected at that time point (Brennan et al., 2006; Kim & Goldie, 2008). Static models include state-transition models (e.g., Markov models) or individual-level microsimulations. Dynamic models include (a) aggregate-level compartmental models wherein transmission dynamics are captured via differential equations, and (b) individual-level simulations, which can include Monte Carlo microsimulations, discrete-event simulations, and ABMs. A systematic review of model-based cost-effectiveness analyses for HCV published in 2016 (Chhatwal et al., 2016) revealed that until then, only static models had been developed for this purpose. However, a number of dynamic models, both compartmental and agent-based, have been developed since the publication of this review.

Given that HCV is an infectious disease, a dynamic model may best capture the impact of an anti-HCV intervention. A number of compartmental differential equation based models have been developed for this purpose, as will be discussed in the next subsection. However, such models do not capture the impact of individual-level heterogeneity on disease-related outcomes, whether at the population or patient level. Further, estimating the uncertainty in model outcomes by incorporating stochasticity into such models is a non-trivial task. These drawbacks are addressed by ABMs, wherein disease spread is modelled via interactions between entities (referred to as agents) that represent members of the population of interest (Willem, 2015). ABMs provide a flexible and comprehensive approach for modelling the dynamics of infectious disease transmission at a sufficiently detailed level. A key challenge associated with the development of ABMs includes availability of reliable data for parameterizing agent interaction models in the environments of interest (Abualkhair et al., 2020; Ghaderi, 2022).

A limited number of agent-based models have been developed for cost-effectiveness analyses for anti-HCV interventions. Extant ABMs have been developed for the United States (He et al., 2016; Ayer et al., 2019), France (Cousien et al., 2015) and the Netherlands (van Santen et al., 2016).

These models focus on HCV transmission among injecting drug users (IDUs). However, in the Indian, and indeed in the broader South Asian and developing world contexts, the bulk of HCV transmissions occur via contaminated medical procedures such as blood transfusions (Lim et al., 2020; Das et al., 2019; Farhan et al., 2023). Building upon preliminary work (Das et al., 2019), this study presents the first ABM developed for the developing world, and indeed the first that explicitly models HCV transmission through modes other than injecting drug use.

Table 1 summarizes the dynamic transmission studies developed for HCV.

Table 1: Summary of dynamic transmission models developed to assess the impact of DAA treatment strategies for HCV. *Abbreviations and acronyms.* S: Single, M: Multiple; W: Within horizon, L: Lifetime horizon, F: Fixed horizon; M1: Injecting drug use, M2: sexual route, M3: Implicit non-injecting drug use, M4: Implicit modelling through risk values, M5: Medical procedures, M6: Community risk, M7: Hemodialysis.

Study	Transmission model	Transmission modes	Disease progression model	Geography of analysis	Uptake rate(s)	Screening/treatment frequencies	Timing of treatment considered	Horizon of health and cost outcomes estimation	Types of outcomes evaluated
Cipriano et al. (2012)	Compartmental	M1, M2	Compartmental	US	S	M	No	L	E,H,C
Martin et al. (2013)	Compartmental	M1	Not incorporated	UK, Canada, Australia	M	S	No	Not carried out	E
Bennett et al. (2015)	Compartmental	M1	DTMC	UK	M	S	No	L	E,H,C
Cousien et al. (2016)	Agent-based	M1	DTMC	France	M	S	No	Not carried out	E
He et al. (2016)	Agent-based	M1, M3	DTMC	US	M	S	No	F	E,H,C
Scott et al. (2016)	Compartmental	M1	DTMC	Australia	M	S	No	W	H,C
van Santen et al. (2016)	Agent-based	M1	DTMC	Netherlands	S	S	No	W	E,H,C
Ayoub & Abu-Raddad (2017)	Compartmental	M4	Not incorporated	Egypt	M	S	No	Not carried out	E
Bennett et al. (2017)	Compartmental	M1	DTMC	UK	M	S	No	L	H,C
Cousien et al. (2018)	Agent-based	M1	DTMC	France	S	S	No	L	E,H,C
Ayer et al. (2019)	Agent-based	M1, M3	DTMC	USA	M	S	No	F	E,H
Lim et al. (2020)	Compartmental	M1, M5, M6	Compartmental	Pakistan	S	M	No	W	E/C
Kwon et al. (2021)	Compartmental	M1	DTMC	Australia	M	S	No	F	E,H,C
Epstein et al. (2023)	Dynamic microsimulation	M1, M7	DTMC	USA	S	M	No	W	E,H,C
This study	Agent-based	M1, M5	DTMC	India	M	M	Yes	L	E,H,C

2.1. Literature Pertaining to ROI : Model-based Cost-effectiveness Analyses of HCV Treatment

The literature relevant to ROI pertains to model-based cost-effectiveness analyses of HCV treatment - in particular, treatment with DAAs.

Studies that involve the use of dynamic models for assessing the impact of DAAs on health and economic outcomes are the most relevant to this study. He et al. (2016) developed an ABM for HCV transmission through injecting drug use, and then assumed that a certain proportion of transmission occurs via an aggregate mode referred to as ‘other than injecting drug use’. This model was then used to evaluate the cost-effectiveness of risk-based and universal opt-out screening

policies in prisons. This simulation model was later used by Ayer et al. (2019) to test index-based policies, developed through restless bandit modeling, for prioritizing treatment for HCV patients in prisons. Ayoub & Abu-Raddad (2017) studied the impact of treatment on HCV epidemiology and health economic outcomes via a deterministic aggregate compartmental model set in Egypt, and considered injecting drug use and blood transfusions as transmission modes. More recently, Epstein et al. (2023) employed an individual-level modeling approach for HCV transmission among a fixed cohort of hemodialysis patients wherein HCV infections are introduced in dialysis centers via injecting drug use among patients.

The only dynamic model set in South Asia, in our knowledge, is described in Lim et al. (2020): a compartmental model set in Pakistan to model creation of new HCV infections through not only injecting drug use, but also via medical procedures and tattooing. Being an aggregate model, it did not explicitly model individual-level interactions for disease transmissions. In the Indian context, aside from preliminary work underpinning this study (Das et al., 2019), the relevant studies are all static models that do not consider HCV transmission (Aggarwal et al., 2017; Goel et al., 2018; Chugh et al., 2019, 2021). These studies incorporate a disease progression discrete-time Markov chain (DTMC) that simulates the progression of the disease to evaluate the impact of different DAA regimes on the health and cost outcomes. Given that the models did not incorporate the creation of new infections, the secondary benefits of treatment in preventing new infections could not be estimated.

Only a few studies, in our knowledge, have quantified the effects of stepping up treatment uptake on cost and health outcomes (He et al., 2016; Bennett et al., 2017; Ayer et al., 2019; Lim et al., 2020). In fact, we identified only one study that addressed a question relevant to *RO1*: quantify the impact of not considering transmissions on the cost-effectiveness of DAAs: Bennett et al. (2017). The authors used a deterministic compartmental model to capture HCV transmission in a population of IDUs. The study reports the impact of neglecting transmissions on treatment cost-effectiveness at multiple treatment uptake rates. The authors found that the cost-effectiveness of adopting DAAs over previous treatment regimens with lower cure rates improved with increasing uptake rate when transmissions are included. In the Indian context, the studies of Chugh et al. (2019) and Chugh et al. (2021) explored the effects of increasing treatment uptake rates on DAA cost-effectiveness, but with static DTMC based models. With respect to these studies, and in particular Bennett et al. (2017), we see that dynamic individual-level models that consider the inherent stochasticity in disease transmission and spread, and therefore also characterize the

uncertainty around their estimated outcomes, have not been developed: (a) for the South Asian or Indian contexts and more broadly for the developing world; (b) that consider modes of transmission other than injecting drug use; (c) and to answer the research questions we consider as part of *RO1* (mentioned previously in Section 1). Thus our research contributions pertaining to *RO1* involve addressing the above gaps.

2.2. Literature Pertaining to RO2: Impact of Intervention Frequency and Timing

We found limited work that assesses the cost-effectiveness of changing frequency and timing of interventions for HCV. This appears to be the case for other infectious diseases as well, with relevant studies being conducted in deterministic settings - for example, Duijzer et al. (2018) for influenza via a compartmental model, and Deo et al. (2015) for HIV via a hybrid compartmental and integer programming model.

For HCV, Cipriano et al. (2012) evaluates screening strategies among injecting drug users undergoing opioid replacement therapy. The authors found that more frequent screening strategies are more cost-effective. Contrastingly, Epstein et al. (2023) studied multiple screening frequencies on individuals undergoing hemodialysis, and reported that lower screening frequencies were more cost-effective. Both studies only modelled creation of new HCV infections through the injecting drug use route. The studies also did not analyze the epidemiological, health and economic impact of timing of screening and/or treatment during the study time horizon.

Therefore, our research contribution with respect to *RO2* involves estimating the epidemiological, health and economic impact of *both* the timing and frequency of HCV treatment with DAAs as a function of treatment uptake rate, accomplished via an ABM developed for the South Asian and developing world contexts that explicitly incorporates HCV transmission via modes other than injecting drug use. Importantly, our study also highlights the trade-off between the ‘optimal’ policy in terms of its cost-effectiveness and its epidemiological effectiveness in terms of the number of infections created.

2.3. Literature Pertaining to RO3: Outcomes Estimation in Agent-based Models

Two types of studies are commonly found in terms of the time horizon over which outcomes pertaining to cost-effectiveness analyses are evaluated (Basu & Maciejewski, 2019). The first involves assessment of outcomes only within the duration of the intervention deployment period - these are called *within-trial horizon* analyses. In the context of an ABM, this would typically mean that outcomes for agents are assessed only until the end of the model execution time horizon.

Alternatively, outcomes are assessed for a duration beyond the intervention deployment period. For ABMs, this often involves estimating outcomes for agents of interest for their lifetimes. Such analyses are called *lifetime horizon* analysis. We suggest a third type - *fixed horizon* analysis: one where outcomes are assessed beyond the end of the intervention deployment period and up to a certain pre-specified point of interest, but not for the entire duration of individual lifespans. Conducting lifetime horizon analyses with ABMs is challenging, as the execution of the disease progression model for agent lifespans for the entire agent cohort (typically large in size) may be computationally expensive or challenging to implement (the latter because termination points are likely to differ for each agent). Thus these studies are often *within-trial* or *fixed horizon analyses*. To address this, an outcomes allocation approach - e.g., assigning expected values of outcomes (e.g., quality-adjusted life years) generated from the DTMC model of the disease natural history - has also been used. However, this approach does not capture the stochasticity inherent in the progression of the disease. Implementing a stochasticity-preserving outcomes allocation approach within an ABM is a nontrivial task, as one has to consider how the sample path of an agent changes after an initial allocation - e.g., if an infected agent gets cured, and an initial allocation is made upon infection. If one allocates again at the point of change in the sample path (e.g., due to cure), how does one account for outcomes accumulated until this point? Discounting of outcomes also requires careful handling, as the reference point for discounting changes with each agent.

Many relevant studies (see Table 1) do not explicitly mention the exact method used for outcomes estimation, especially when a DTMC is used to simulate HCV natural history. In cases where they do, this approach is often an uncertainty-free one-time allocation of average outcomes generated by repeated multiplication of the transition probability matrix for the DTMC with the state distribution vector (starting from an initial distribution) for a fixed time period, as in Bennett et al. (2017). Alternatively, outcomes estimation is done for fixed cohorts. We see similar approaches for outcomes estimation for agent-based models developed for other diseases as well, such as in HIV (Gopalappa et al., 2017) and HPV (Olsen & Jepsen, 2010).

In this study, as part of our research contribution associated with $RO\beta$, we propose a new and computationally more efficient approach, with theoretical grounding, for estimating the lifetime outcomes for agents of interest within an ABM that removes the need for executing the natural history DTMC (NH-DTMC) model beyond the end of the intervention deployment period. This approach takes into account changes in agent sample paths by integrating accumulated outcomes between points of change in agent sample paths with outcomes allocated at points of change. We

call this approach the *outcomes allocation* (OA) method for *lifetime horizon* outcomes estimation.

3. Agent-Based Simulation Model Development

The ABM that we develop to accomplish research objectives 1 through 3 consists of the following components, each of which we describe in this section.

1. Agent interaction environments and ancillary dynamics (e.g., agent demographic model, model run settings).
2. Disease progression module.
3. Treatment module.
4. Outcomes estimation module.

3.1. Agent Interaction Environments and Ancillary Dynamics

Two agent interaction environments were incorporated into the model, corresponding to the dominant modes of transmission in the Indian context: a medical environment and a social interaction environment. The medical environment was chosen based on a study by Chakravarti et al. (2013) that reported the key modes of transmission for HCV in the Indian context. The authors found that 74.1% of HCV infections were caused via unsafe medical procedures, which included blood transfusions, injections, dental procedures and surgeries. Injecting drug use was the next major mode of transmission, accounting for nearly 16% of infections, which we incorporated as part of the social interaction environment. Chakravarti et al. (2013) also found that 9% of infections were caused via unsafe tattooing practices. However, we were unable to obtain sufficiently reliable publicly available information regarding this mode of transmission, and hence we did not explicitly incorporate this environment. Instead, given that the spread of HCV via tattooing is also due to needle-stick injuries, similar to injecting drug use, we modified certain parameter estimates associated with the social interaction environment to incorporate this transmission mode.

In addition, a dynamic agent cohort is incorporated, meaning agents enter and exit the model via birth and death during the simulation execution period. The simulation execution period was divided into two parts: the first 50 years of simulation time, called the calibration period, and then 10 years where the intervention (different treatment models with DAAs) was introduced and outcomes of interest were collected for analysis. The calibration period ensured that at the point in the simulation execution period when collection of outcomes of interest begins, demographics of

the agent cohort and the spread of HCV in terms of its prevalence matched those documented in the literature relevant for validating the model. A 10 year intervention period was chosen as a time scale sufficient to capture impacts of different interventions at a population level. Further, daily time points were used so that interactions relevant to the spread of the disease could be captured with the appropriate granularity.

The model was initialized with 40,000 agents at the beginning of the calibration period. Among this cohort, 15 IDUs and 5 infected agents were included. Only agents between the ages of 23 and 102 were included. These demographic attributes were chosen for initializing the agent cohort based on preliminary experiments conducted to ensure that the required agent cohort demographics and HCV spread were achieved at the end of the calibration period. Average annual birth and death rates of 15 and 6 per 1,000 persons, respectively, were used in the model, with the death rates decomposed into lower and higher death rates for older and younger agents, respectively.

3.1.1. Medical environment for HCV transmission.

In this environment, two types of agents interact: medical professionals and ‘normal’ agents from the general population. On a given day, each agent may visit the medical environment with a certain probability, where they interact with a medical professional who, again with a certain probability, may follow unsafe clinical practices. If an infected agent visits such a medical professional, then that particular professional’s environment gets contaminated. Thus, other uninfected agents who visit that medical professional on that day may get infected. This interaction model is depicted in Figure 1a.

The above interaction model needs to be parameterized with the appropriate agent-specific probabilities. This includes, for example, the daily probability of an agent visiting the medical environment, the probability that a medical professional employs unsafe clinical practices, and the probability that an uninfected agent gets infected from a contaminated medical environment.

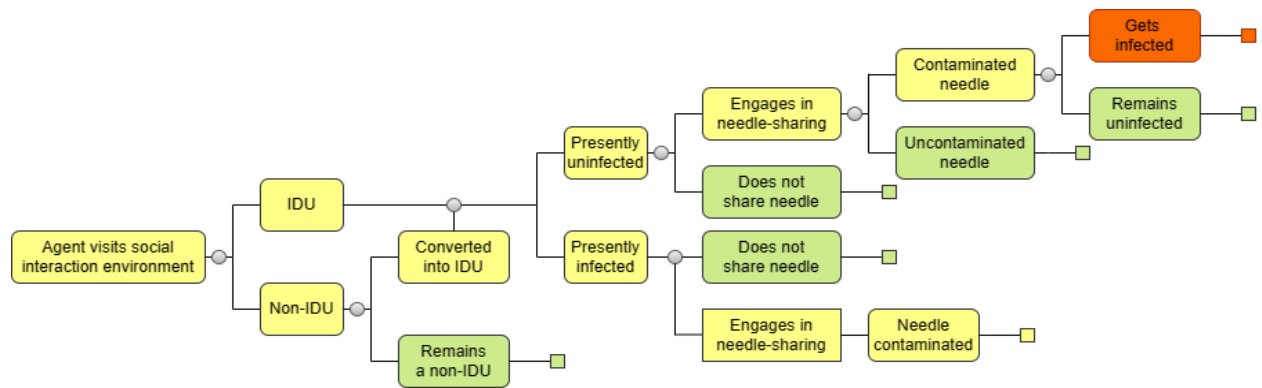
The daily probability of an agent visiting the medical environment (denoted by q_v^{med}) was estimated via the annual per-capita average numbers of the relevant procedures in the Indian context - injections, surgeries, dental procedures and blood transfusions. q_v^{med} is estimated via equation 1 below.

$$q_v^{med} = \frac{m_i + m_b + m_s + m_d}{360} \quad (1)$$

In equation 1, m_j denotes the annual average number of times the j^{th} medical event of interest occurs, where $j \in \{\text{injections } (i), \text{ blood transfusions } (b), \text{ surgeries } (s), \text{ dental procedures } (d)\}$. The



(a) Agent interactions in the medical environment.



(b) Agent interactions in the social interaction environment.

Figure 1: Agent interaction models in the HCV dynamic transmission model.

proportion of medical procedures that were unsafe in the Indian context (q_{uns}^{med}) was estimated from Pala et al. (2016), which indicated that nearly half the clinics across the country did not follow safe sterilization practices, and thus q_{uns}^{med} was set to 0.50. Next, the number of agents seen by a medical professional on a given day, denoted by $N_{p|mp}$, was estimated using the doctor-patient ratio ($r_{d|p}$), reported to be 1:1800 (see Table 2). We thus derived $N_{p|mp}$ using the relation $N_{p|mp} = \frac{q_v^{med}}{r_{d|p}}$. The number of medical professionals was increased with time in accordance with the increase in population.

The probability of an uninfected agent acquiring an infection from a contaminated medical environment, denoted by q_t^{med} , was calculated as a weighted average of the respective probabilities of getting infected via a contaminated version of each of the medical procedures considered in the medical environment.

$$q_t^{med} = \frac{\sum_{j \in \{i,b,s,d\}} m_j \times r_j}{\sum_{j \in \{i,b,s,d\}} m_j} \quad (2)$$

In equation 2, r_i , r_b , r_s and r_d the per-event probabilities of contracting an HCV infection due to contaminated injections, blood transfusions, surgeries and dental procedures. Thus, in order to estimate q_t^{med} , we need estimates for each r_j . Estimates for r_i and r_s were available; however, those for r_b and r_d are not. However, Chakravarti et al. (2013) reported that blood transfusions alone accounted for 54% of the HCV load, and thus formed 74% of the contribution of the medical environment. We can thus write:

$$m_b \times r_b = 0.74 \times \sum_{j \in \{i,b,s,d\}} m_j \times r_j \text{ and} \quad (3)$$

$$q_t^{med} = \frac{m_b \times r_b}{0.74 \times (\sum_{j \in \{i,b,s,d\}} m_j)}$$

Thus only an estimate of r_b is required to estimate q_t^{med} . Given that such an estimate was not available from the relevant clinical literature, q_t^{med} was treated as a ‘calibration’ variable, and estimated via the model calibration process (described in section Appendix C).

3.1.2. Social interaction environment.

The social interaction environment was created to incorporate HCV transmissions via injecting drug use. Two key events occur here: a non-IDU can get converted into an IDU, and/or an uninfected IDU gets infected via a needle-sharing event. The interaction model for this environment is depicted in Figure 1b. If an uninfected non-IDU agent visits the environment, they may get converted into an IDU. If an IDU visits the environment, then they may engage in a needle-sharing

event. If an infected IDU is part of the needle-sharing group then we assume that all IDUs that are part of said group are exposed, and may acquire HCV with a certain probability.

Much of the data required to parameterize the above interaction model was obtained from a study by Ambekar & Tripathi (2008) of IDU characteristics in the Indian states of Punjab and Haryana. We assume that a non-IDU visits this environment once a week. The daily probability of an IDU visiting the social interaction environment, denoted by $q_v^{soc,I}$ was estimated using the weekly frequency (e.g., twice a week, thrice a week) of injecting observed among IDUs in the Punjab state (Ambekar & Tripathi, 2008). This was calculated as the weighted average of the injecting frequencies observed in the districts of Punjab, with the weights being the populations of the individual districts. Further, only agents between the ages of 16 and 32 were eligible to become IDUs, based on the observation by Ambekar & Tripathi (2008) that 75% of IDUs were aged between 18 and 30 years. Similarly, the authors also reported that duration for which agents remained as IDUs was 3 years. The size of an IDU group that may engage in a communal injecting event wherein needles may be shared was determined to be 3, based on a study by Azim et al. (2008) in Bangladesh (similar data was not available for the Indian context). Note that an overestimation of the average IDU group size reported in Azim et al. (2008) was made to account for HCV transmission via tattooing, as discussed earlier.

The probability of a non-IDU getting converted into an IDU is estimated by conditioning on whether an agent is unemployed or not. This is because the rate of unemployment among IDUs was observed to be 26%, compared to 16.6% among the general population (Ambekar & Tripathi, 2008; Ministry of Statistics & Programme Implementation, Government of India, 2023). We developed the following model (equation 4) to incorporate the association of unemployment with the probability of a non-IDU being converted into an IDU (denoted by q_c).

$$q_c = q_c^{ue} \times q_{ue}^g + q_c^e \times (1 - q_{ue}^g) \quad (4)$$

Here q_c^{ue} and q_c^e represent the probabilities of an unemployed non-IDU agent versus that of an employed agent getting converted into an IDU. The odds of an unemployed non-IDU getting converted into an IDU as compared to an employed non-IDU was taken as the ratio of the probability of being unemployed for an IDU ($q_{ue}^I = 1 - q_{ue}^g$) to the probability of being unemployed for the general population (q_{ue}^g). Thus, we have: $\frac{q_c^{ue}}{q_c^e} = \frac{(1 - q_{ue}^g)}{q_{ue}^g}$. Estimates for q_{ue}^I and q_{ue}^g were available, but the values of q_c , q_c^{ue} and q_c^e were unknown, yielding three unknown variables and two equations.

Therefore, q_c was also assumed to be a calibration variable. Once its estimate was obtained using calibration, the values of q_c^{ue} and q_c^e were found by applying the above relationships in equation 4.

The probability of having shared needles at least once was reported to be 0.504 by Ambekar & Tripathi (2008). Given an event of the IDU visiting the social interaction on a particular day, we denote the per-event probability of a needle-sharing event among the IDU's group as q_{shar} . However, we could not identify an estimate for q_{shar} from the literature, and hence this also was estimated via model calibration. However, an upper bound of 0.504 guided the calibration process for this parameter.

Finally, the probability of acquiring the HCV infection from using a contaminated needle - i.e., as part of a needle-sharing injecting event among a group of IDUs (of size 3, as discussed earlier) with at least one infected agent - was estimated as 0.02 (Rolls et al., 2012).

The agent-based model input parameters associated with the medical and social interaction environments are provided in Table 2 below.

Table 2: Input parameters for the medical and social interaction environments of the HCV agent-based model.

Environment	Relevant parameter for HCV transmission	Value	Source	
Medical environment	Annual per-capita average number of	Injections, m_i	2.9	IPEN Study Group et al. (2012)
		Blood transfusions, m_b	0.023	NACO (2018)
		Surgeries, m_s	0.009	Weiser et al. (2016)
		Dental procedures, m_d	0.982	Statista (2018)
	Daily probability of an agent visiting the medical environment, q_v^{med}	0.0108	Calculated using equation 1 (section 3.1.1)	
	Doctor to patient ratio, $r_{d p}$	1:1800	Deo (2013)	
	Number of patients per medical professional, $N_{p mp}$	19	Calculated as $\frac{q_v^{med}}{r_{d p}}$	
	Proportion of medical professionals following unsafe practices, q_{ums}^{med}	0.50	Pala et al. (2016)	
	Contribution of medical procedures to HCV infection load	74.10%	Chakravarti et al. (2013)	
	Per-event probability of infection from blood transfusion, r_b	0.806	Calibrated	
Per-event probability of infection in the medical environment, q_t^{med}	0.0064	Calibrated		
Social interaction environment	Proportion of IDUs in the age range of 18-30 years	75%	Ambekar & Tripathi (2008)	
	Age range of IDUs in the model	16-32 years	Age-wise uniformly distributed	
	Daily probability of an IDU visiting the environment	0.486	Ambekar & Tripathi (2008)	
	Daily probability of a non-IDU visiting the environment	0.142	Weekly visits assumed	
	Probability of an IDU being unemployed, q_{ue}^l	0.26	Ambekar & Tripathi (2008)	
	Probability of a non-IDU agent being unemployed, q_{ue}^g	0.166	Indiaspend (2017)	
	Probability of conversion of a non-IDU into an IDU for an	employed agent, q_c^e	1.44×10^{-5}	Calibrated
		unemployed agent, q_c^e	2.25×10^{-5}	Calibrated
	Duration for which an IDU remains an IDU	3 years	Ambekar & Tripathi (2008)	
	Size of an IDU network	3 persons	Based on Azim et al. (2008)	
	Probability of an IDU having shared a needle at least once	0.504	Ambekar & Tripathi (2008)	
	Per-event needle sharing probability in a network of size 3, q_{shar}	0.41	Calibrated	
	Per-event probability of getting infected due to sharing needles, q_t^{shar}	0.02	Rolls et al. (2012)	

With regard to the disease progression module of the ABM, we use a validated DTMC for modelling HCV progression that has been widely used in cost-effectiveness studies of interventions for HCV (Ayer et al., 2019). This model has been used in all the studies which evaluated the cost-effectiveness of DAAs in the Indian context (Aggarwal et al., 2017; Goel et al., 2018; Chugh et al.,

2019, 2021). We refer to this model henceforth as the NH-DTMC, and its implementation within the ABM for each infected agent can be considered as the execution of a Monte Carlo simulation replication. A detailed description of the NH-DTMC and its implementation for each infected agent (Algorithm 4) is provided in Section Appendix A.

3.2. Treatment Module for Infected Agents

Treatment was considered only for agents for whom treatment had not failed earlier given that with DAAs, the probability of treatment failure is low (Chugh et al., 2019). DAAs are the current standard of care in India, as in much of the rest of the world. Chugh et al. (2019) estimated real-world cure or SVR rates for DAAs from their experience of treating HCV patients in Indian Punjab. The authors found that the pan-genotypic combination treatment of DAAs sofosbuvir (SOF) and velpatasvir (VEL) yielded the highest SVR rates, and hence we used SOF+VEL as the standard of care in our simulation experiments, with genotype-specific SVR rates (ranging from 84% to 86%) sourced from Chugh et al. (2019).

We now discuss how the treatment is applied to the agent cohort in the intervention period. First, we recall that the simulation execution period is divided into two stages: a calibration period of 50 years of simulation time during which the demographics of the agent cohort and the spread of the HCV infection reach levels corresponding to the validation targets (published real-world observations of HCV prevalence). A 10-year intervention period then begins during which treatment using DAAs is applied to a subset of infected agents and outcomes pertaining to HCV epidemiology and its health and cost impacts are recorded.

In this study, we evaluate multiple treatment models or approaches towards the treatment and management of HCV. These involve varying the timing and frequency of treatment - for example, running treatment camps once every 3 years, or at the beginning of the intervention period versus the end of the intervention period. Each of these alternate treatment models are compared against the default model that represents the status quo and is referred to henceforth as the *annual-treatment* model. This treatment model, under which an increasing proportion of infected agents are treated every year (hence the name), represents the status quo in the following way. We assume that, based on inputs from our clinical collaborator with field experience in managing HCV treatment in a high-prevalence area, beginning from a base value of the proportion of the infected cohort who receive treatment (capturing the impact of initial awareness regarding HCV), public awareness regarding HCV increases every year. The number of infected agents who

receive treatment via implementation of the default *annual-treatment* model over the intervention period is controlled by the target *uptake rate*. For example, if the target uptake rate is set to be 10%, then our implementation of *annual-treatment* attempts to ensure that 10% of all infected agents present from the beginning of the intervention period (including those infected during the calibration period) to the end of the intervention period are treated.

We now discuss the approach towards implementing the *annual-treatment* model so that the target uptake rate is achieved. Given that some infected agents die before undergoing treatment, hence the target uptake rate is not precisely achieved during a given simulation run. Further, the naive approach of treating 10% of infected agents every time period (e.g., a year) would not capture the scenario of increasing numbers of infected agents receiving treatment every year. Therefore, we designed an algorithm that, starting from a base proportion of infections treated, takes into account the new infections created every year and steps up the proportion treated every year to achieve the target uptake rate. The algorithm that we design for this purpose may be more broadly applicable: it can be used, in a dynamic transmission model such as an ABM or an ordinary differential equation based compartmental model, to implement any intervention that needs to be gradually stepped up over regular time points to achieve a preset coverage rate. In a compartmental model, our algorithm can be used with a constant intervention effectiveness rate applied to the relevant compartment (e.g., the ‘infected’ compartment in an SEIR model) within the model. We carried out all our simulation experiments on treatment of HCV using SOF+VEL at six target treatment uptake rates- 10%, 30%, 50%, 70%, 90% and 95%.

The implementation of the annual treatment model is described in Algorithm 1 below. In this model, treatment takes place at discrete time points across a time horizon (e.g., every day over a period of one week or in our case, every year across a 10-year intervention period). We assume that new infections take place at the beginning of the time point, then treatment takes place for a certain proportion of the then (living) infected population. After treatment, the remaining infections result in new infections in the following time point. We do not consider non-disease-related deaths while outlining the algorithm for the sake of simplicity.

Notation

- j, i = Time indices.
- N_j^{new} = Number of new infections caused at time point j .
- N_j^a = Number of new infections caused at time point j which are assigned for treatment.
- N_{j_1, j_2}^{Tr} = Number of new infections caused at time point j_1 which are treated at time point j_2 .

j_2 , where $0 \leq j_1 \leq j_2 \leq n$.

– M_j^{Tr} = Number of infections treated at time point j .

– M_j^l = Number of infections assigned to treatment remaining untreated after treatment has concluded at time point j .

– n = Number of time points in the intervention period.

– N^0 = Number of initial infections, or the number of infections at the beginning of the intervention period.

– $u \in [0, 1]$ = Target uptake rate of the treatment or the proportion of patients assigned to treatment.

– $\alpha \in [0, 1]$ = Initial coverage rate or proportion of the initial pool of infected patients assigned to treatment who undergo treatment at the beginning of the intervention period.

Algorithm 1 Implementation of the annual-treatment model.

```

for  $j = 0 \rightarrow n$  do
  if  $j = 0$  then
     $N_j^{new} = N^0$ 
  else
     $N_j^a = u \times N_j^{new}$ 
    if  $j = 0$  then
       $M_j^{Tr} = \alpha \times N_j^a$ 
    else
       $M_j^{Tr} = \left[ \alpha + (1 - \alpha) \times \frac{j}{n} \right] \times (M_{j-1}^l + N_j^a)$ 
      where  $M_{j-1}^l = \sum_{i=0}^{j-1} N_i^a - \sum_{i=0}^{j-1} M_i^{Tr}$ 
    end if
  end if
end for

```

In Algorithm 1, $j = 0$ is the beginning of the period and $j = n$ is the end of the intervention period, with treatment occurring over $n + 1$ time periods. If u is the target uptake rate across the intervention period, then we assume that a fraction α of u (e.g., 30% of all those to be treated, which may be, say, 10% of all infected agents present across the intervention period) are treated at the end of $j = 0$. The coverage of treatment in each time period is then scaled upwards linearly to reflect the likelihood of awareness increasing with time. In each time period $j > 0$, we assign $u\%$ of newly created infections to be treated (N_j^a), and then set the number treated in j to the coverage fraction $\left[\alpha + (1 - \alpha) \times \frac{j}{n} \right]$ multiplied by the total number of infections present at j , which is the sum of the number of infections remaining at the end of $j - 1$ (M_{j-1}^l) and N_j^a . Note that if $\alpha \times u$ fraction of the infections present prior to $j = 1$ are treated at $j = 0$, then scaling up the coverage

linearly implies that with each time period, a fraction of the remaining coverage (equal to $1 - \alpha$) to be achieved must be added to the base coverage at $j = 0$, α . To ensure that coverage at $j = n$ is equal to u (or in other words, $\alpha = 1$), this fraction is set to $\frac{j}{n} \times (1 - \alpha)$.

Due to page length constraints, further details of the annual treatment model is described in detail in Section Appendix B. There, we provide a numerical illustration of the implementation of Algorithm Appendix B, as well as a straightforward analytical argument to show that it achieves the desired uptake rate without non-disease-related mortality.

3.3. Outcomes Estimation Module

Prior to describing the estimation of outcomes, we point the reader to section Appendix C, where we describe the validation of the simulation model.

3.3.1. Outcomes of interest.

The outcomes generated by the model are of three types: epidemiological outcomes such as HCV antibody and RNA prevalences, as discussed in section Appendix C; health outcomes such as life-years (LYs) and quality-adjusted life-years (QALYs); and economic outcomes such as the average total costs of HCV incurred per agent (infected and uninfected - these are *population-level* outcomes) and the average total costs of HCV incurred per chronically infected patient (*patient-level* outcomes). In addition, a summary measure of the cost-effectiveness of the intervention under consideration called the net monetary benefit (NMB) is also generated as a function of the above health and economic outcomes.

The generation and validation of epidemiological outcomes is discussed in section Appendix C. We now discuss the generation of *lifetime horizon* health and economic outcomes, and our novel approach towards generating these efficiently within a dynamic transmission model such as an ABM.

Outcomes such as the LYs for each agent are generated by simply recording the time spent by the agent in the model and in each disease state. QALYs associated with each state are estimated by multiplying a utility weight capturing the health-related quality of life associated with the health state (ranging between 0.0 for death and 1.0 for perfect health) with the time spent in the state. Summing this product across all states (including the uninfected state) yields the QALYs associated with each agent in the model. HCV health state costs are similarly estimated: the recurring and fixed costs incurred by being in a given health state are aggregated along with the resource use (e.g., the frequency of resource use - weekly, monthly) and time spent in the state to yield the costs

associated with the health state. These are then summed across each state to yield the total costs associated with the management of HCV for an infected agent. We note here that only the direct medical costs associated with managing HCV are incorporated in our analysis, such as the costs of treatment, physician visits, diagnostics and monitoring, surgeries and hospitalizations.

The benchmark approach towards estimating LYs, QALYs and costs for each infected agent would involve executing the NH-DTMC and the non-disease-related mortality (non-DRD) models every time step, recording the LYs (length of one time step - e.g., one day or year), QALYs and costs incurred in the time step, and adding it to the outcomes accumulated until the previous time step. This process would have to be repeated until the agent dies or reaches the maximum permissible age. This termination time point may extend well beyond the ABM execution time horizon. We refer to this process as the *incremental accumulation* (IA) outcomes estimation process, and depict it in Algorithm 2 below. Note that Algorithm 2 calls Algorithm 4.

Notation:

- t : time index, wherein t may extend beyond the ABS time horizon T .
- $a_t \in \{1, 2, \dots, A\}$: age group that the agent belongs to at time t .
- Inf_t : infection status of the agent at time t ; $Inf_t = 1$ if infected, 0 otherwise.
- $k_t \in \{1, \dots, K\}$: disease stage/state at t .
- Q : outcome of interest.
- Q_t^I : Incrementally accumulated value of Q^I until t .
- ΔQ_t^I : incremental value of Q^I at time t .
- *Init*: subroutine that assigns initial values of agent a_t , Inf_t and k_t for the agent.
- *Eval*: subroutine that calculates ΔQ_t^I to be added to Q_{t-1}^I based on a_t and $Inf_t \times k_t$. If uninfected, then $Inf_t \times k_t = 0$, and if infected, $Inf_t \times k_t = k_t \in \{1, \dots, K\}$.
- *Updt*: subroutine that updates Inf_t and k_t based on the transmission and progression modules.

In order to calculate the above outcomes, we needed estimates of utility weights and HCV-related costs incurred in the Indian context. We obtained utility weights for HCV health states from Chugh et al. (2019), who used HCV health state utility weights estimated specifically for the Indian context. Distinct from Chugh et al. (2019), we applied utility weights for the uninfected health state as well in order to capture the deterioration of quality of life with age. In other words, if $u_i \in (0, 1)$ is the utility weight for uninfected agents of the i^{th} age group ($i \in I$), and $u_k \in (0, 1)$ ($k \in K$) is the utility weight for the k^{th} HCV health state, then the utility weight for an infected agent of age group i in health state k is $u_i \times u_k$. The age-group specific utility weights

Algorithm 2 The *incremental accumulation* approach for *lifetime-horizon* outcomes estimation.

```

 $t \leftarrow 0$  ▷  $t$  is the point of call of this algorithm for an agent.
 $a_0, Inf_0, k_0 \leftarrow Init(a, Inf, k)$ 
 $Q_0^I \leftarrow 0$ 
while Agent is alive do ▷ Updates occur at the end of  $t$ 
   $t \leftarrow t + 1$ 
   $a_t \leftarrow a_{t-1}$  ▷ Update age group
   $Inf_t, k_t \leftarrow Updt(Inf, k)$  ▷ Call Algorithm 4
   $\Delta Q_t^I \leftarrow Eval(a_t, Inf_t \times k_t)$ 
   $Q_t^I \leftarrow Q_{t-1}^I + \Delta Q_t^I$ 
end while
Return  $Q_t^I$ 

```

are obtained from He et al. (2016).

The resource use and costs associated with the management of HCV were obtained from our expert clinical collaborator whose team has been involved in the management and surveillance of HCV in Punjab over multiple decades. The utility weights capturing the age-related deterioration in quality of life by age group and HCV disease state are provided in Table D.10 and the HCV resource use and management costs are provided in Table D.11. Discounting is applied to the health and economic outcomes generated by the model, wherein LYs, QALYs and costs are discounted at 3% per year, based on the Indian health technology assessment guidelines (Prinja et al., 2018).

We now describe our proposed methodology for efficient generation of *lifetime horizon* outcomes in dynamic transmission models.

3.3.2. The OA outcomes estimation algorithm.

Consider the calculation of *lifetime horizon* outcomes for an agent of interest - i.e., one who becomes infected - in the HCV ABS. We assume that this agent is born during the execution of the model (alternatively, the agent may be part of the cohort at model initiation) and becomes infected at some time t , where $t < T$ and T is the time point corresponding to the end of the model execution period. Given that HCV is a slow-moving disease that does not affect patient life expectancy on average, and T in our case is less than the average life expectancy of an Indian person, it is likely that this agent will be alive at the end of T . Now, because cost-effectiveness analyses typically (and ideally) require *lifetime horizon* outcomes, this implies that estimating LYs, QALYs and disease-related costs for this agent would involve executing the NH-DTMC and the non-DRD model for this agent until their death or they reach the maximum permissible age considered in this model. If many such agents are present at T , including relatively young agents infected just prior to T ,

this will involve executing the disease progression DTMC and the non-DRD models for every such agent well beyond T , when the execution of the agent-based component of the model stops. This can incur substantial computational expense, which in the case of agent-based models adds to an already considerable computational overhead. A similar process - execution of the non-DRD model alone beyond T - would have to be followed for uninfected agents alive at the end of T as well, because our goal is to estimate population-level outcomes, and not restrict our analysis to infected agents alone.

Given the above context, we propose a method, which we refer to as the *outcomes allocation* (OA) method, to alleviate this computational expense by eliminating the need for execution of the NH-DTMC and the non-DRD models beyond T . The OA method involves utilizing outcomes incrementally accumulated and recorded during model execution as well as outcomes randomly sampled and allocated to agents from a repository of outcomes generated and stored based on agent age and disease status as a one-time exercise.

Before we explain the OA algorithm, we briefly describe the creation of the outcomes repository. As mentioned earlier, the repository was created as a one-time execution of the NH-DTMC and the non-DRD models. In order to generate the repository, a cohort of one million agents was created with an age distribution similar to that of the Punjab state in 2011. Given the large size of the cohort, a sufficiently large number of agents of all ages relevant to the analysis were present in the cohort. For infected agents, we executed the NH-DTMC and the non-DRD models (see Algorithm 4) for each infected agent assuming they have started their sojourn in one of the ten disease states of interest. For uninfected agents, we executed the non-DRD model assuming they have just started their sojourn in one of the A age groups. For example, we execute the NH-DTMC and the non-DRD models assuming an infected agent has just transitioned to the F0 HCV stage (state); and for uninfected agents, they have just begun their sojourn in age group a . Note that the Markovian assumption underlying the model of disease progression implies that the amount of time spent in the state prior to execution of these models does not need to be taken into consideration. This process is then repeated for each of the ten HCV states of interest, and for each case, the LYs, QALYs and HCV-related costs for each agent in the cohort are recorded. The same process is repeated for the estimation of discounted outcomes as well. The generation of the repository for each initial state requires 7.7 minutes of computation time on our workstation (Intel Xeon processor with clock speed 3.4 GHz and 32 GB random access memory), and hence the generation of the entire repository required 77 minutes.

In order to sample and allocate outcomes from the repository for an agent of a given age a and disease state k , we first extract a subset of outcomes from the repository corresponding to agents of age a and disease state k , and then randomly sample (with replacement) LYs, QALYs and HCV-related costs from this sub-repository and allocate them to the agent under consideration.

The OA approach is described in Algorithm 3. Its premise is simple: we are interested only in the distributions of the outcomes under consideration and their moments, and hence the outcomes of individual agents are not of interest and may be allocated randomly as long as they are sampled appropriately. Therefore, for each agent in the model, infected or uninfected, we allocate outcomes randomly based on their age and/or disease state. Note that we allocate outcomes to agents who remain uninfected throughout the model execution period. This is because interventions such as treatment also prevent new infections over and above curing those infected, thereby improving the health outcomes of the population at large, which then need to be measured.

Algorithm 3 The *outcomes allocation* method for generating *lifetime horizon* outcomes for agent-based simulations.

```

Initialize  $t = 0$ , agent age as  $a_0$ , and simulation run length  $T$ .
Initialize infection status  $Inf \in \{0, 1\}$  w.p.  $p$ .  $Inf = 1 \implies$  infected; otherwise uninfected.
If  $Inf = 1$ , then record disease state  $k$  ( $k \in \{1, 2, \dots, K\}$ ).
Initialize accumulated outcomes  $L_I, Q_I, C_I = 0$ .
Define function  $Rep$  that randomly samples and allocates outcomes  $L_A, Q_A, C_A$  from repository
based on composite health state  $v = (Inf \times k, a)$ .
Define function  $Inc$  that increments outcomes  $L_I, Q_I, C_I$  in each time point based on composite
health state  $(Inf \times k, a)$ .
Allocate initial outcomes by sampling from repository:  $L_A, Q_A, C_A = Rep(L_{A(0)}, Q_{A(0)}, C_{A(0)} \mid$ 
 $(Inf \times k, a))$ .
for  $t = 0 : T$  in increments of  $\delta t$  do
    Update  $Inf \leftarrow Inf'$ 
    Update  $a \leftarrow a + \delta a$ 
    if  $|Inf' - Inf| > 0$  then
         $L_A, Q_A, C_A = Rep(L_{A(t)}, Q_{A(t)}, C_{A(t)} \mid Inf' \times k', a)$ 
         $L, Q, C = L_A + L_{I(t)}, Q_A + Q_{I(t)}, C_A + C_{I(t)}$ 
    else
        if  $Inf' = 1$  then
             $k \leftarrow k'$ 
        end if
    end if
     $L_{I(t)}, Q_{I(t)}, C_{I(t)} = Inc(L_{I(t+\delta t)}, Q_{I(t+\delta t)}, C_{I(t+\delta t)} \mid Inf' \times k, a)$ 
     $Inf = Inf'$ 
    if agent dies then
        return  $L, Q, C$ 
    end if
end for

```

Thus, the OA algorithm randomly samples and allocates outcomes to each agent at their entry into the model, depending upon their age and/or disease state. The algorithm then records and accumulates the outcomes of each agent incrementally with each passing time step - i.e., similar to the incremental accumulation (IA) approach - during the model execution period. Further, each time the infection status of an agent changes - that is, if an infected agent is cured or an uninfected agent is infected - a fresh set of outcomes is randomly sampled and allocated to the agent. In this case, however, the new set of outcomes are added to the incrementally accumulated outcomes associated with the agent under consideration.

Now, we provide theoretical grounding for the comparability of the OA and the IA methods for outcomes estimation. The argument involves considering the various sample paths that agents undertake within the ABM - e.g., entry into the model upon birth or model initiation, infection, cure, and model exit via death. For a representative sample path, under a mild assumption, we prove the required result - i.e., that the OA and IA methods yield the same expected values for the outcomes in question.

Notation.

- S : Set of possible sample paths for an agent; $S = \{1, 2, \dots, \hat{S}\}$; s = sample path index.
- $(a, Inf \times k)$ = composite health state tuple; $a \in$ set of age groups $\{1, 2, \dots, A\}$, where A = age group with maximum allowable age; Inf = infection status, where $Inf = 1$ if infected, 0 if uninfected; $k \in$ set of DTMC disease states $\{1, 2, \dots, K\}$, K = number of disease states. $a_{(l)}$ and $a_{(u)}$ are the bounding (lower and upper) ages contained in age group a .
- V = Number of $(a, Inf \times k)$ health state tuples; v = index of health states, $v \in \{1, 2, \dots, V\}$.
- N_{sv} = Number of agents of sample path s whose final allocations were done in health state v .
- τ_M = discrete random variable capturing the number of model time steps spent alive by an agent, counting from the time of final outcome allocation under the OA algorithm.
- j : Agent index, $j \in \{1, 2, \dots, N\}$.

We state the below assumption regarding the construction of the age group set.

Assumption 1. Let $a_{i(l)}$ and $a_{i(u)}$ ($a_{i(l)} < a_{i(u)}$) be the bounding ages contained in age group a_i ($a_i \in \{1, 2, \dots, A\}$), with $w_i = a_{i(u)} - a_{i(l)}$. Let T_{l_s} be the expected lifespan of an agent with sample path s . Then $\forall a_i \in \{1, 2, \dots, A\}, w_i \ll T_{l_s}$.

We consider an example sample path for an agent to develop the analytical argument. An agent is born uninfected at t_0 , and allocation A_0 is made when the agent is in health state $v_0 = (a_0, 0)$. The agent then gets infected at t_1 , and allocation A_1 is made when the agent enters health state

$v_1 = (a_1, 1)$. The agent is then cured at t_2 , and allocation A_2 is made when the agent enters health state $v = (a_2, 0)$. The agent exits the model at T without further change in infection status, and the most recent outcome (allocated at t_2) A_2 , summed with the incremental outcome C_2 recorded for the agent until t_2 , is returned as its outcome for statistical analysis. a_1 and a_2 represent the age groups that the patient belongs to at time points t_1 and t_2 , respectively.

Let $Q_{j,s,v}^{OA}$ be the outcome returned by the j^{th} agent via the OA algorithm assuming they follow the above sample path s , and whose final outcome was allocated when the agent entered health state v . $Q_{j,s,v}^{OA}$ will be the sum of the outcome allocated at t_2 when they enter health state v , denoted by $A_{j,2}^{sv}$ and the outcome incrementally accumulated until t_2 , which is $C_{j,2}$.

$$Q_{j,s,v}^{OA} = C_{j,2} + A_{j,2}^{sv} \quad (5)$$

We do not include the dependence on s and v for $C_{j,2}$ because it is recorded in the same way regardless of the health state and sample path an agent experiences.

Now, if the outcome is calculated via the incremental accumulation approach (denoted at the agent level by Q_j^I), then $Q_j^I = C_{j,T_j}$. In this expression, T_j denotes the termination point of the incremental outcome accumulation process for the j^{th} agent (i.e., at death of the agent), which may extend well beyond the ABM execution time horizon T . This termination point is likely to be different for each agent, hence its indexation by j . This can be broken down as follows:

$$Q_j^I = C_{j,T_j} = C_{j,2} + C_{j,2+} \quad (6)$$

Here, $C_{j,2+}$ represents the value of the outcome accumulated incrementally from t_2 onwards. This decomposition of Q_j^I around t_2 is done to facilitate comparison with $Q_{j,s,v}^{OA}$.

We now state and prove the following result.

Proposition 1. *The difference between the expected value of the outcome returned by the OA algorithm (Algorithm 3) for the j^{th} agent under sample path s , $E[Q_{j,s,v}^{OA}]$, and that returned by the incremental accumulation method (Algorithm 2), $E[Q_j^I]$, is a function of the time spent in the age group of the agent at the point of final allocation.*

Proof. $E[Q_{j,s,v}^{OA}] = E[Q_j^I] \iff E[C_{j,2} + A_{j,2}^{sv}] = E[C_{j,2} + C_{j,2+}]$. By the linearity of addition of expectations, this implies that we need to show that $E[A_{j,2}^{sv}] = E[C_{j,2+}]$. For this, we need to consider how $A_{j,2}^{sv}$ is generated (and allocated) and how $C_{j,2+}$ is calculated.

$C_{j,2+}$ is calculated from the point of cure t_2 of the agent by execution of Algorithm 2. At t_2 the agent has just entered the health state tuple v . In this case, the agent may already have spent some time, say τ ($\tau \in [0, w_2)$), in the age group a_2 prior to t_2 . w_2 is the width of age group a_2 .

$A_{j,2}^{sv}$ is randomly sampled from the repository stratified by tuple v , which in this case is $(a_2, 0)$. Each component of the vector of samples of the outcome in the repository is generated assuming that the agent begins in the age group $a_2 \in \{1, 2, \dots, A\}$ and disease state 0, where 0 represents the uninfected/HCV-free state.

Now, we consider the process of generating each realization of $A_{j,2}^{sv}$ and $C_{j,2+}$. The vector of outcome samples from which $A_{j,2}^{sv}$ is randomly sampled is generated by executing the NH-DTMC and the non-DRD models, via execution of Algorithm 2, assuming the agent enters the v^{th} health state. $C_{j,2+}$ is also generated by execution of Algorithm 2. Thus, if $\tau = 0$, then the random experiments that generate the realizations of the random variables, $A_{j,2}^{sv}$ and $C_{j,2+}$ will be the same, implying the random variables $A_{j,2}^{sv}$ and $C_{j,2+}$ will also be identically distributed. However, because in general $\tau \neq 0$, we need to examine the outcomes produced by the OA and IA algorithms further.

In general, $A_{j,2}^{sv}$ and $C_{j,2+}$ are functions of: (a) the time spent in each disease state, which is a vector τ_K with elements τ_k ($k \in \{1, 2, \dots, K\}$); and (b) the time spent alive τ_M - both considered from the point of allocation (OA) / accumulation (IA). For the particular sample path s that we are considering, since the agent is cured at t_2 , τ_K need not be considered. Thus only the random variable τ_M needs to be considered in the calculation of $E[A_{j,2}^{sv}]$ and $E[C_{j,2+}]$. Given the discrete conceptualization of time in the ABM setting, τ_M can be modeled as a discrete random variable. Also, because we impose a maximum age limit A_u for each agent, the sample space for τ_M is finite.

Let τ_M^{OA} and τ_M^{IA} represent the versions of τ_M generated by the OA and IA algorithms, respectively. Then the sample spaces for τ_M^{OA} and τ_M^{IA} can be written as $\chi_{OA} = \{0, 1, 2, \dots, L\}$ and $\chi_{IA} = \{0, 1, 2, \dots, L - \tau\}$. Here L represents the maximum number time steps from t_2 for which an agent can remain alive given the imposition of the upper age limit A_u . Let $p = \{p_0, p_1, \dots, p_L\}$ and $q = \{q_0, q_1, \dots, q_{L-\tau}\}$ be the *pmfs* for τ_M^{OA} and τ_M^{IA} , respectively, where each $p_i \geq 0$ ($i \in \chi_{OA}$), $q_1 \geq 0$ ($i \in \chi_{IA}$) and $\sum_{i=0}^L p_i = 1$ and $\sum_{i=0}^{L-\tau} q_i = 1$. Here $p_i = P(\tau_M = a_{2(l)} + i | \tau_M \geq a_{2(l)})$, $i \in \chi_{OA}$ and $q_i = P(\tau_M = a_{2(l)} + \tau + i | \tau_M \geq a_{2(l)} + \tau)$, $i \in \chi_{IA}$. Then we can write $E[A_{j,2}^{sv}]$ and $E[C_{j,2+}]$ as follows:

$$\begin{aligned} E[A_{j,2}^{sv}] &= \sum_{i=0}^L i \times p_i \\ E[C_{j,2+}] &= \sum_{i=0}^{L-\tau} i \times q_i \end{aligned} \tag{7}$$

From equation 7 and the above argument, it is clear $|E[A_{j,2}^{sv}] - E[C_{j,2+}]|$ is a function of τ . This

completes the proof. A similar argument can be constructed for all sample paths $s \in S$. \square

The difference in outcome expected values between the OA and the IA methods will be substantial only if τ is comparable in magnitude to L . This arises only if a_2 is close to A . Given the large value of A_u , the use of year-long age groups, and the age-group specific probabilities implemented in the case of our simulation, only a negligibly small proportion of agents reach the age group A , justifying the use of Assumption 1. Thus in the case of our simulation, under Assumption 1, $\tau \ll L$ for almost every agent, implying $L - \tau \cong L$, which in turn means that $\chi_{OA} \cong \chi_{IA}$ and $p \cong q$. This yields $E[A_{j,2}^{sv}] \cong E[C_{j,2+}]$.

We now consider the expected value of the outcome generated by the simulation across all sample paths. For this, we first consider the average value of the outcome generated from a replication under use of the OA method, which is used to estimate its expected value. This is denoted by $\bar{Q}^{OA} = \frac{\sum_{j=1}^N Q_j^{OA}}{N}$. Denoting $\sum_{j=1}^N Q_j^{OA}$ by Q_{tot}^{OA} , we can decompose this by the sample paths that agents experience within the simulation as well as the health states at which the final allocation is made for each agent within a given sample path. That is:

$$Q_{tot}^{OA} = \sum_{s=1}^S \sum_{v=1}^V \sum_{j=1}^{N_{sv}} Q_{j,s,v}^{OA}$$

The above expression for Q_{tot}^{OA} can be rewritten as follows:

$$Q_{tot}^{OA} = \sum_{s=1}^S \sum_{v=1}^V N_{sv} \times \bar{Q}_{j,s,v}^{OA}$$

Here $\bar{Q}_{j,s,v}^{OA}$ is the average outcome estimated across the set of agents under sample path s and whose final allocation was done when they were in health state v . Treating N_{sv} as a constant without loss of generality, we can rewrite the above equation as follows:

$$Q_{tot}^{OA} = N_{sv} \times \sum_{s=1}^S \sum_{v=1}^V \bar{Q}_{j,s,v}^{OA}$$

Invoking the strong law of large numbers, the expected value of Q_{tot}^{OA} can then be written as follows:

$$E[Q_{tot}^{OA}] = N_{sv} \times \sum_{s=1}^S \sum_{v=1}^V \lim_{n \rightarrow \infty} \frac{\sum_{j=1}^n Q_{j,s,v}^{OA}}{n} \quad (8)$$

An expression similar to equation 8 can be written for the expected value of the outcome estimated from the incremental accumulation approach. This is given below.

$$E[Q_{tot}^I] = N_{sv} \times \sum_{s=1}^S \sum_{v=1}^V \lim_{n \rightarrow \infty} \frac{\sum_{j=1}^n Q_{j,s,v}^I}{n} \quad (9)$$

At this point, we recall from equations 5 and 6 that for agents under sample path s and whose final allocation occurs at health state v , $Q_{j,s,v}^{OA} = Q_{j,s,v}^{OA} = C_{j,2} + A_{j,2}^{sv}$, and $Q_{j,s,v}^I = C_{j,2} + C_{j,2+}$. Using these relationships in equations 8 and 9, we can write:

$$E[Q_{tot}^{OA}] = N_{sv} \times \sum_{s=1}^S \sum_{v=1}^V \lim_{n \rightarrow \infty} \frac{\sum_{j=1}^n (C_{j,2} + A_{j,2}^{sv})}{n} \quad (10)$$

$$E[Q_{tot}^I] = N_{sv} \times \sum_{s=1}^S \sum_{v=1}^V \lim_{n \rightarrow \infty} \frac{\sum_{j=1}^n (C_{j,2} + C_{j,2+})}{n}$$

Under Assumption 1, we have proved in Proposition 1 that $A_{j,2}^{sv}$ and $C_{j,2+}$ are identically distributed. Hence we can replace $A_{j,2}^{sv}$ with $C_{j,2+}$ in the expression for $E[Q_{tot}^{OA}]$ in Equation 10, which gives us $E[Q_{tot}^I]$. Note that, as in the proof of Proposition 1, we prove that the expected values of the outcomes in question are equal by proving a stronger result - namely, that the outcomes from both methods are identically distributed. Further, in the context of the simulation, the *iid* replicate values of $Q_{j,s,v}^{OA}$ and $Q_{j,s,v}^I$ that are used to compute $\bar{Q}_{j,s,v}^{OA}$ and $\bar{Q}_{j,s,v}^I$, respectively, in Equation 10 are represented by the the outcomes of agents who experience sample path s and whose final allocation occurs in health state v .

We now state Proposition 2 that summarizes the result we have derived above.

Proposition 2. *The expected values $E[Q^{OA}]$ and $E[Q^I]$ of the average values of the outcomes \bar{Q}^{OA} and \bar{Q}^I returned by a single replication of the ABM under the OA (Algorithm 3) and the IA methods (Algorithm 2), respectively, are equal.*

3.3.3. Numerical verification of the OA algorithm.

We now present the results of the experiments conducted to validate the OA algorithm. We ran one replication of the simulation at five target treatment uptake rates (implemented via the annual treatment algorithm [Algorithm 1]) with both methods: the OA and the IA approaches. The same random number seed was used for both sets of experiments. Discounted and undiscounted LYs,

QALYs and costs as well as computational runtimes associated with the OA and IA approaches were compared. We ran the experiments on a workstation with an Intel Core i7-8700 processor, 32GB installed memory and 3.20 *GHz* clock speed. The results from the experiments are provided in Table 3 below.

Table 3: Results of validating the *outcomes allocation* approach for outcomes estimation.

Outcome	10%		30%		50%		70%		90%	
	IA	OA								
Runtime (seconds)	121662	29331	108443	24573	105493	25576	104801	24305	111383	26741
Life years	70.51	70.00	70.6	70.09	70.72	70.17	70.81	70.24	70.86	70.24
Discounted life years	27.17	27.13	27.18	27.14	27.19	27.14	27.19	27.14	27.18	27.12
QALYs (years)	59.78	59.17	59.96	59.34	60.16	59.51	60.32	59.65	60.42	59.71
Discounted QALYs (years)	23.76	23.67	23.81	23.72	23.87	23.77	23.91	23.81	23.93	23.82
Costs (INR)	29691	30308	23862	24304	17152	17572	12013	12257	8110	8740
Discounted costs (INR)	12367	12487	10103	10188	7612	7699	5602	5682	4174	4307

We see from the above results that the outcomes from both approaches are almost identical. There is a marginal underestimation of outcomes generated by the OA approach when compared to the IA approach. This is partly because we executed the NH-DTMC and the non-DRD models using annual time steps to speed up the generation of the samples, while we executed the ABS using daily steps. Further, when the allocation was done, a sample corresponding to $a + 1$ years of age was allocated to an agent who was between a and $a + 1$ years.

With regard to runtimes, we see that while the mean runtime for one run of the IA approach required 110,348 seconds with a standard deviation of 6,822 seconds, the mean runtime for one run of the OA approach required 26,105 seconds with a standard deviation of 2,042 seconds. This implied an average reduction of 76.3% in runtimes with the OA approach. Moreover, as mentioned earlier, the generation of the repository was a one-time exercise and required around 77 minutes (4620 seconds).

4. Computational Experiments for Research Objectives 1 and 2

In this section, we describe the computational experiments associated with research objectives 1 and 2 and their results.

For both *RO1* and *RO2*, the epidemiological outcomes considered were the HCV antibody, HCV *RNA*, and IDU prevalences at the end of the intervention period. Health outcomes considered

include life years and QALYs, and economic outcomes include the direct medical costs associated with the management of the HCV infection. Both undiscounted and discounted estimates of health and economic outcomes were generated. Health and economic outcomes were generated at both the *population-level* as well as at a *patient-level*. Population-level outcomes were generated by dividing estimates of health and economic outcomes by the total number of agents in the simulation model. Patient-level outcomes were estimated by considering the number of chronically infected agents in the model.

The cost-effectiveness of an intervention considered in the model (e.g., treatment ‘camps’ every 5 years with an uptake rate of 50%) was summarized using the net monetary benefit. Given that our model incorporates transmissions, the NMB for a given intervention was calculated for population-level outcomes alone, as it would account for costs and health outcomes gained by preventing transmissions by curing HCV patients. The NMB of an intervention is calculated as the incremental health benefits gained in terms of QALYs, converted to monetary terms, minus the incremental costs incurred when the intervention is implemented. The NMB calculation is provided in equation 11 below.

$$NMB = k \times (Q_n - Q_s) - (C_n - C_s) \quad (11)$$

In equation 11, k represents the willingness-to-pay threshold for incremental health benefits, commonly estimated as three times the per-capita annual gross domestic product of the country where the analysis is situated (Prinja et al., 2018). Q_n and Q_s represent the QALYs associated with the intervention and the status quo, respectively, and C_n and C_s represent the costs. The per-capita GDP of India was INR 113,967 in 2022-23 (Ministry of Statistics & Programme Implementation, Government of India, 2023). In almost all cases, the ‘status quo’ intervention against which the NMB of an intervention was calculated was the annual treatment model as described in 1 with a target uptake rate of 10%.

The computational experiments for *ROs* 1 and 2 were carried out on multiple workstations with varying capacity: workstations with Intel Core-i7 and Xeon processors with clock speeds ranging from 3.2 GHz to 3.4 GHz and random access memories of 16GB, 32GB, and 64GB, respectively. The runtimes per replication ranged from 4.2 hours to 7.8 hours, respectively, for the most and least powerful workstations.

4.1. Research Objective 1: Quantifying the Impact of Treatment Uptake and Incorporating Transmissions on DAA Cost-effectiveness

We first investigated the impact of increases in treatment uptake rate, from 10% to 95%, on epidemiological, health and economic outcomes associated with HCV treatment with DAAs. The results of this experiment are documented in Table 4.

Table 4: Impact of treatment uptake rate on the cost-effectiveness of directly-acting antivirals. Standard deviations in parentheses.

Target treatment uptake rate (%)	10%	30%	50%	70%	90%	95%
Effective treatment uptake rate (%)	9.5 (0.2)	29 (0.6)	47.7 (0.2)	67.05 (0.8)	84.9 (0.2)	89.2 (0.5)
Epidemiological outcomes						
HCV Antibody prevalence (%)	6.2 (0.2)	5.6 (0.06)	5.1 (0.07)	4.6 (0.02)	4.1 (0.08)	4.0 (0.04)
HCV RNA prevalence (%)	4.4 (0.1)	3.2 (0.05)	2.2 (0.08)	1.4 (0.05)	0.7 (0.04)	0.6 (0.01)
IDU prevalence (%)	0.08 (0.01)	0.08 (0.02)	0.07 (0.01)	0.05 (0.01)	0.04 (0.01)	0.05 (0.003)
Health and economic outcomes						
<i>Population-level outcomes</i>						
Life years	70.00 (0.04)	70.12 (0.03)	70.19 (0.04)	70.28 (0.04)	70.30 (0.05)	70.33 (0.03)
Life years (discounted)	27.15 (0.02)	27.15 (0.01)	27.15 (0.01)	27.15 (0.01)	27.13 (0.01)	27.13 (0.01)
QALYs (years)	59.15 (0.03)	59.36 (0.02)	59.52 (0.04)	59.68 (0.03)	59.76 (0.05)	59.80 (0.02)
QALYs (years, discounted)	23.67 (0.01)	23.73 (0.01)	23.78 (0.01)	23.82 (0.01)	23.84 (0.01)	23.84 (0.01)
Costs (INR)	31469 (1009)	24684 (362)	18206 (755)	12700(489)	8287 (397)	7223 (176)
Costs (INR, discounted)	12935 (390)	10302 (132)	7899 (282)	5812 (137)	4160 (128)	3780 (43)
Net monetary benefit (NMB)	0	23147	42645	58408	66898	67278
<i>Patient-level outcomes</i>						
Life years	71.04 (0.46)	72.87 (0.43)	75.10 (0.17)	77.10 (0.40)	78.50 (0.32)	78.95 (0.65)
Life years (discounted)	39.10 (0.21)	39.93 (0.19)	41.07 (0.08)	42.20 (0.21)	43.12 (0.33)	43.37 (0.28)
QALYs	48.15 (0.35)	51.58 (0.41)	55.37 (0.15)	58.90 (0.27)	61.76 (0.40)	62.56 (0.48)
QALYs (discounted)	27.68 (0.19)	29.30 (0.19)	31.15 (0.06)	32.96 (0.17)	34.38 (0.32)	34.88 (0.23)
Costs	795230 (4699)	676428 (2696)	543451 (10942)	420211 (15172)	303418 (10759)	270807 (6330)
Costs (discounted)	326869 (1227)	282326 (1172)	235821 (3261)	192304 (4052)	152358 (3167)	141703 (1614)

With regard to epidemiological outcomes, we observe that, as expected, increasing treatment uptake rate leads to substantial decreases in HCV antibody as well as RNA prevalence. In fact, up to (and including) an uptake rate of 90% the rate of decrease in these prevalences actually increases with increase in uptake rate, implying epidemiological benefits to be gained with improving uptake rate even for treatment programmes performing reasonably well (e.g., uptake rates around 75%). We also see these benefits reflected in epidemiological dynamics across the intervention period: for example, the HCV antibody prevalence increased from 3.6% to 6.2% at the end of the intervention period with the 10% uptake rate, whereas it increased from 3.6% to 4.1% with the 90% uptake rate. However, limited epidemiological gains are observed when the uptake rate exceeds 90% - for example, the decrease in HCV antibody prevalence is not statistically significant when uptake rate increases from 90% to 95%.

When population-level health and economic outcomes are considered, increasing treatment uptake is cost-effective at all uptake rates exceeding 10%, as all NMB estimates are positive. However, increasing uptake rate yields only marginal changes in population-level life years and QALYs. This

is not surprising given that: (a) across all the outcomes in Table 4, the maximum HCV antibody prevalence at the end of the intervention period, which indicates the extent to which the population has been affected, is only 6.2% (at the lowest uptake rate of 10%); and (b) even among this small set of infected agents, chronic HCV does not, on average, impact life expectancy. On the other hand, we see significant savings in costs and corresponding increases in the NMB estimates with increasing uptake. The rate of increase in the NMB, however, decreases with increasing uptake.

An important question arises here: in resource-constrained settings, how do we quantitatively determine the point beyond which efforts to increase uptake rate may cease? We suggest that this question may be answered by calculating the NMB associated with each uptake rate assuming that the comparator is the largest uptake rate smaller than the uptake rate in question. This is expressed in equation 12 below.

$$\begin{aligned}
 NMB(u_i) &= k \times (Q(u_i) - Q(u_j)) - (C(u_i) - C(u_j)) \quad \forall u_i \in U \\
 \text{where } U &= \{u_1, u_2, \dots, u_K\}, \quad u_j = \max\{u_k : k \neq i, u_k < u_i\} \\
 \text{and } u_i &\neq \min U
 \end{aligned} \tag{12}$$

In equation 12, we assume that there are K uptake rates (where $K = |U|$), and the NMB is calculated for the i^{th} uptake rate u_i , assuming that $u_{i-1} = \max\{u_j : j \neq i, u_j < u_i\}$, without loss of generality. We propose that the ‘critical’ uptake rate, which may be denoted by u^* can be determined as the uptake rate at which $NMB(u_i)$ falls below some predetermined threshold T_{NMB} . A natural choice for T_{NMB} is 0, which is often the threshold used to characterize a given health intervention as being cost-effective or not (Prinja et al., 2018). This is expressed in equation 13 below.

$$u^* = \arg \min_{u_i \in U} \{NMB(u_i) | NMB(u_i) \geq T_{NMB}\} \tag{13}$$

The $NMB(u_i)$ values are provided in Figure 2 below for each uptake rate greater than 10%. It is clear that there appears to be limited health economic benefit to be gained by increasing u_i beyond 95%. We acknowledge, however, that assessing the value of expanding (reimbursable) access to treatment to even one additional person requires careful judgement and involves a certain degree of subjectivity. This is reflected in the fact that T_{NMB} in equation 13 must still be specified by the analyst/policymaker.

At the patient level, there is a substantial, statistically significant improvement in all outcomes (health outcomes increase and costs decrease) as uptake rate increases. The rates of change of LYs

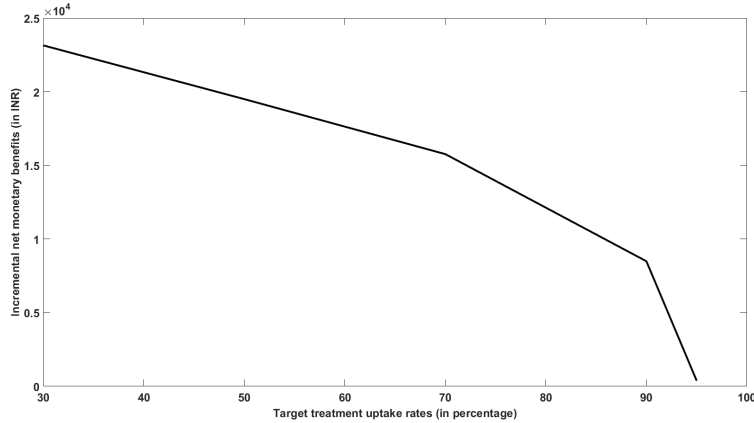


Figure 2: Incremental net monetary benefit at each applicable treatment uptake rate, calculated with respect to the previous uptake rate.

and QALYs are convex, peaking at 50% and decreasing with further increase in uptake rate - once again indicating diminishing returns. The most striking result is the improvement in QALYs – an improvement of 30.0% in undiscounted QALYs and 26.0% in discounted QALYs, reaffirming that increasing penetration of treatment among those chronically infected leads to more significant gains in quality of life than in life expectancy itself.

The above outcomes clearly suggest that efforts to increase treatment uptake rate, up to a certain threshold, yield substantial epidemiological, health and economic benefits. Our analysis suggests an approach (expressed in equations 12 and 13) for determining the critical uptake rate beyond which incremental health economic benefits are minimal.

We now discuss outcomes that quantify the extent to which incorporating transmissions impacts the cost-effectiveness of HCV treatment. These outcomes were obtained by stopping transmissions during the intervention period of a given simulation run. This involved modifying the values of the transmission-related parameters - for example, the probability of an IDU influencing a non-IDU into becoming an IDU is set to zero. All other simulation settings are retained, and the outcomes from this simulation experiment are depicted in Figure 3. In Figure 3, we plot the ratios of (a) the NMBs from the WT to the WoT analyses, (b) the costs from the WoT to the WT analyses (for ease of comparison with the other ratio plots), and (c) the QALY terms from the NMB equation for the WT and the WoT cases. It is clear that in all cases, the ratios converge to 1 as the treatment uptake rate increases. The numerical outcomes corresponding to Figure 3 are provided in Table 5 below.

We see that, for all uptake rates, the NMBs from the *with transmission* (WT) case are signif-

Table 5: Impact of treatment uptake rate - *without* incorporating transmissions in the analysis - on the cost-effectiveness of directly-acting antivirals. Standard deviations in parentheses.

Target treatment uptake rate (%)	10%	30%	50%	70%	90%	95%
Effective treatment uptake rate (%)	9.0 (0.4)	27.7 (0.7)	46.7 (0.6)	65.7 (0.8)	83.5 (0.2)	87.5 (0.4)
<i>Population-level outcomes</i>						
Life years	70.15 (0.04)	70.17 (0.04)	70.23 (0.05)	70.29 (0.04)	70.30 (0.03)	70.35 (0.03)
Life years (discounted)	26.94 (0.01)	26.96 (0.01)	26.99 (0.01)	27.02 (0.01)	27.04 (0.01)	27.05 (0.01)
QALYs (years)	59.53 (0.03)	59.58 (0.03)	59.66 (0.04)	59.74 (0.03)	59.80 (0.02)	59.84 (0.02)
QALYs (years, discounted)	23.63 (0.01)	23.66 (0.01)	23.70 (0.01)	23.74 (0.01)	23.77 (0.01)	23.79 (0.01)
Costs (INR)	16233 (156)	13813 (173)	11350 (301)	8860(160)	6384 (47)	5833 (139)
Costs (INR, discounted)	6646 (72)	5829 (47)	4998 (99)	4156 (38)	3324 (27)	3137 (28)
Net monetary benefit	0	11074	25581	40099	51188	58213
<i>Patient-level outcomes</i>						
Life years	68.99 (0.45)	71.03 (0.43)	73.65 (0.27)	76.10 (0.56)	77.86 (0.24)	78.53 (0.62)
Life years (discounted)	38.53 (0.24)	39.81 (0.22)	41.23 (0.16)	42.61 (0.24)	43.70 (0.22)	44.02 (0.3)
QALYs (years)	46.00 (0.36)	49.50 (0.35)	53.45 (0.13)	57.29 (0.47)	60.60 (0.28)	61.46 (0.63)
QALYs (years, discounted)	26.99 (0.23)	28.85 (0.21)	30.81 (0.12)	32.75 (0.24)	34.46 (0.22)	34.88 (0.32)
Costs (INR)	814580 (4020)	692810 (8891)	569150 (13223)	444425 (7936)	320057 (3031)	292583 (9115)
Costs (years, discounted)	333493 (1194)	292370 (1562)	250647 (3950)	208454 (1345)	166623 (320)	157317 (2316)

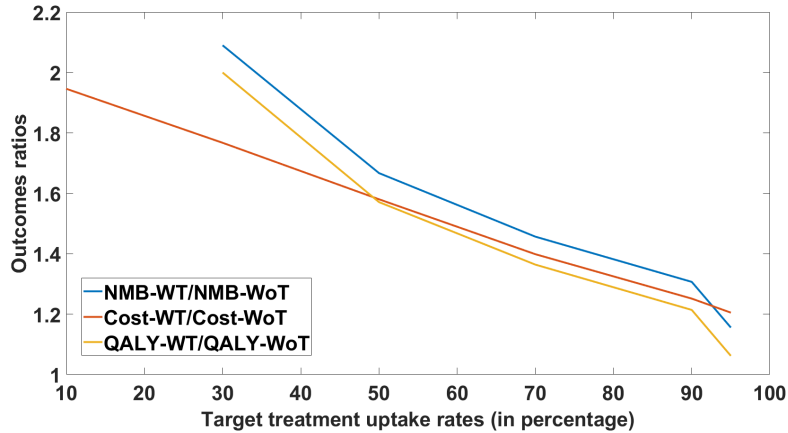


Figure 3: Ratios of outcomes - net monetary benefits (NMBs), costs and the QALY terms within the NMB equation - for the with transmission (WT) and the without transmission (WoT) analyses.

icantly larger than those from the *without transmission* (*WoT*) case. In fact, we see that for the 30% uptake rate case, the NMB for the *WT* case is more than double the *WoT* case. The ratio of the NMBs for the *WT* and *WoT* cases decreases with increase in uptake rate and approaches one. This is expected, as with an uptake rate of 100%, no transmissions are possible given that all HCV patients are treated. Thus, the key insight that emerges from this experiment is that incorporating transmissions into assessments of the cost-effectiveness of HCV treatments is vital especially when treatment uptake rates are low (e.g., $< 50\%$), as is the case in India (CDC, 2024).

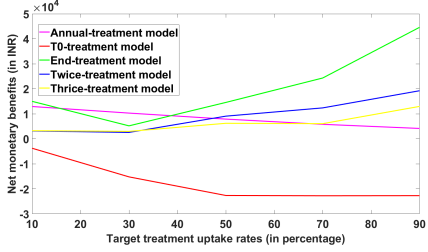
We also observe that medical costs are significantly higher in the *WT* case - at a 10% uptake rate, we see that the ratio between the discounted medical costs for the *WT* case to that of the *WoT* case is 1.95, and decreases to 1.25 when the uptake rate is 90%. This increase in medical costs when transmissions are considered is due to the fact that more infections are created and therefore more patients are also treated. The question then arises as to how the NMBs are substantially larger for the *WT* case when compared to the *WoT* case. Two factors drive this. First, for a given uptake rate, the health gains (improvement in QALYs) - with respect to the default uptake rate (10%) - are higher for the *WT* case than those for the *WoT* case. Secondly, we recall that the NMBs for each uptake rate associated with the *WT* and *WoT* cases are calculated with respect to the outcomes associated with 10% annual treatment uptake rate for the same case, and not with respect to the other *WT/WoT* case. Therefore, in addition to the improved health outcomes for the *WT* case, we also see that the medical cost savings achieved at a population level when treatment uptake rate is increased is substantially larger for the *WT* case than for the *WoT* case.

We conclude the above discussion by reiterating that when treatment uptake rates are low, accounting for HCV transmissions in any assessment of the health and economic benefits of HCV treatment is vital.

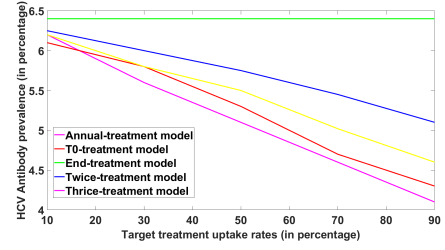
4.2. Research Objective 2 Outcomes: Impact of Timing and Frequency of Treatment

In this section, we discuss the outcomes of the computational experiments conducted to quantify the impact of varying the timing and frequency of treatment of a slow-moving disease such as HCV - i.e., outcomes associated with *RO2*.

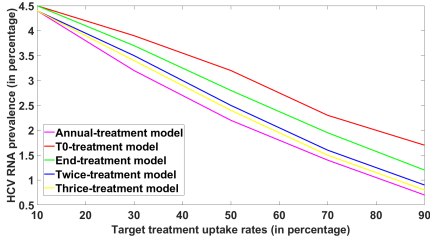
We consider four alternatives to the default *annual – treatment* model, which represents the status quo treatment model, where awareness regarding HCV increases with time and more patients seek treatment. These alternatives to the *annual-treatment model* function as *camp models*, wherein population-wide treatment camps (including facilities for disease screening) are held once every few



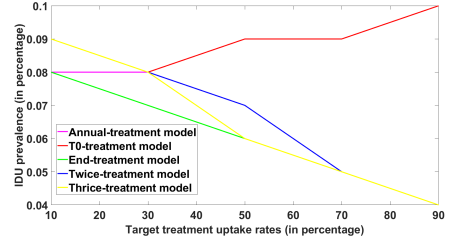
(a) NMBs for alternate treatment models calculated against the *annual-treatment model*.



(b) HCV antibody prevalence.



(c) HCV RNA prevalence.



(d) IDU prevalence.

Figure 4: Epidemiological outcomes and NMBs associated with multiple treatment models as a function of treatment uptake rate

years. We implemented four types of camp models:

1. Treat only at the beginning (T_0 -treatment model). Here, a certain proportion of all infected agents living at the beginning of the intervention period are treated at that time point. Agents that get infected during the intervention/surveillance period are not treated.
2. Treat only at the end (*end-treatment* model). Here, a certain X% of all infected agents living at the end of the intervention/surveillance period are treated at that time point.
3. Treat twice (*twice-treatment* model). Here, X% of all infected agents living at the end of the fifth year and the tenth (final) year of the intervention/surveillance period are treated.
4. Treat thrice (*thrice-treatment* model). Here, X% of all infected agents living at the end of the third, sixth year and the tenth (final) year of the intervention/surveillance period are treated.

Epidemiological outcomes and NMBs associated with the above treatment models are provided in Figures 4a through 4d, and supporting patient-level outcomes are provided in Table 6 below. In Figure 4a, we plot the NMBs of each alternative treatment model calculated against the default *annual-treatment* model.

It is evident from Figure 4a that the T_0 -treatment model is the least cost-effective model. This implies that instituting screening and treatment programmes - especially when resources are limited - at the beginning of a surveillance period is not optimal in terms of NMBs. In fact, for a slow-moving disease such as HCV, such a model is clearly inferior in comparison to the *end-treatment*

Table 6: Patient-level health and economic outcomes of treatment models varying in timing and frequency of treatment.

Target treatment uptake rate (%)	10%	30%	50%	70%	90%
<i>Annual-treatment model</i>					
Effective uptake rate (%)	9.47 (0.23)	28.98 (0.64)	47.72 (0.16)	67.05 (0.84)	84.89 (0.19)
Life years	71.04 (0.46)	72.87 (0.43)	75.10 (0.17)	77.10 (0.40)	78.50 (0.32)
Life years (discounted)	39.10 (0.21)	39.93 (0.19)	41.07 (0.08)	42.20 (0.21)	43.12 (0.33)
QALYs	48.15 (0.35)	51.58 (0.41)	55.37 (0.15)	58.90 (0.27)	61.76 (0.40)
QALYs (discounted)	27.68 (0.19)	29.30 (0.19)	31.15 (0.06)	32.96 (0.17)	34.38 (0.32)
Costs	795230 (4699)	676428 (2696)	543451 (10942)	420211 (15172)	303418 (10759)
Costs (discounted)	326869 (1227)	282326 (1172)	235821 (3261)	192304 (4052)	152358 (3167)
<i>T₀-treatment model</i>					
Effective uptake rate (%)	4.57 (0.23)	14.82 (0.79)	26.81 (0.68)	42.02 (1.07)	57.92 (0.24)
Life years	70.25 (0.37)	71.44 (0.25)	72.69 (0.24)	74.36 (0.70)	75.66 (0.50)
Life years (discounted)	38.89 (0.18)	39.57 (0.16)	40.34 (0.15)	41.27 (0.28)	42.15 (0.28)
QALYs (years)	46.97 (0.26)	48.92 (0.27)	51.02 (0.20)	53.77 (0.54)	56.42 (0.41)
QALYs (years, discounted)	27.22 (0.14)	28.23 (0.16)	29.34 (0.15)	30.74 (0.25)	32.19 (0.24)
Costs (INR)	827360 (6353)	764390 (6566)	685218 (5449)	598367 (13420)	492137 (8066)
Costs (INR, discounted)	340248 (1707)	318469 (2045)	290972 (798)	260994 (3624)	223742 (2121)
<i>End-treatment model</i>					
Effective uptake rate (%)	8.99 (0.19)	27.26 (0.86)	45.23 (0.83)	63.21 (0.88)	80.26 (0.65)
Life years	71.07 (0.48)	73.32 (0.47)	75.52 (0.33)	77.74 (0.34)	80.01 (0.17)
Life years (discounted)	39.29 (0.21)	40.63 (0.23)	41.97 (0.19)	43.29 (0.21)	44.58 (0.16)
QALYs (years)	48.03 (0.32)	51.55 (0.39)	54.99 (0.28)	58.49 (0.29)	61.93 (0.14)
QALYs (years, discounted)	27.74 (0.15)	29.56 (0.20)	31.39 (0.16)	33.22 (0.18)	34.96 (0.13)
Costs (INR)	802047 (7271)	685585 (1856)	575212 (4786)	459706 (6202)	354235 (4084)
Costs (INR, discounted)	331108 (2237)	292039 (541)	254975 (1193)	215820 (1256)	181015 (842)
<i>Twice-treatment model</i>					
Effective uptake rate (%)	9.1 (0.2)	28 (0.6)	47.2 (0.2)	66.05 (0.25)	83.4 (0.3)
Life years	70.95 (0.41)	73.16 (0.36)	75.41 (0.21)	77.52 (0.23)	79.24 (0.42)
Life years (discounted)	39.16 (0.16)	40.31 (0.17)	41.52 (0.10)	42.80 (0.17)	43.92 (0.20)
QALYs (years)	47.98 (0.28)	51.62 (0.23)	55.37 (0.06)	58.90 (0.19)	61.92 (0.37)
QALYs (years, discounted)	27.67 (0.12)	29.46 (0.12)	31.33 (0.05)	33.19 (0.14)	34.81 (0.18)
Costs (INR)	801867 (9231)	681207 (8684)	553402 (11234)	431301 (4697)	318328 (5344)
Costs (INR, discounted)	329832 (3262)	287584 (1936)	243102 (2396)	200589 (251)	162769 (2645)
<i>Thrice-treatment model</i>					
Effective uptake rate (%)	9.6 (0.4)	28.6 (0.4)	47.8 (0.3)	66.3 (0.3)	84.3 (0.2)
Life years	71.20 (0.35)	73.13 (0.44)	75.57 (0.23)	77.70 (0.34)	79.30 (0.36)
Life years (discounted)	39.20 (0.20)	40.21 (0.22)	41.45 (0.17)	42.62 (0.18)	43.69 (0.17)
QALYs (years)	48.21 (0.25)	51.74 (0.35)	55.63 (0.14)	59.13 (0.20)	62.22 (0.32)
QALYs (years, discounted)	27.74 (0.16)	29.47 (0.19)	31.36 (0.14)	33.14 (0.13)	34.80 (0.16)
Costs (INR)	800832 (1189)	673218 (1728)	547292 (4250)	433358 (11311)	311842 (4572)
Costs (INR, discounted)	328994 (1158)	284055 (2129)	239060 (1590)	199271 (3114)	158583 (1117)

model in terms of economic outcomes. From Table 6, it can be seen that the default *annual-treatment* model yields the least costs; however, it also yields the lowest per-patient QALYs as well compared to the other models (except the T_0 -*treatment* model).

From Figure 4a, it is evident that if resource constraints exist such that only one screening and treatment camp can be held during a surveillance period for a disease with a progression profile similar to HCV, treating at the end of the surveillance period is more beneficial. However, the speed of spread of the disease in question is also important here. In our modeled scenario, HCV is not only slow-progressing but also relatively slow in its spread: for example, under the *end-treatment* model, without any treatment for a period of 10 years, we see that HCV antibody prevalence increases from 3.6% to only 6.4%, which corresponds to an approximately 6% annual increase in the number of infections. Alternatively, for a disease that spreads or progresses faster, an intervention such as the *end-treatment* model may not be sufficiently (cost-) effective. Thus the optimal timing of screening and treatment for a disease will depend on its speed of progression as well as speed of spread.

With regard to the frequency of treatment, it is immediately apparent that all treatment models other than the T_0 -*treatment* model yield positive NMBs in comparison to the default model. This implies that the treatment camp model - whether it is conducted twice, thrice or once at the end of a 10-year period - is superior (in NMB terms) to conducting it every year, especially if the diagnosis and treatment rate for HCV is low without screening or awareness programmes. Among these camp models, the *end-treatment* model appears to be the most effective, with its NMBs outstripping the other models especially as uptake rates increase (e.g., beyond 30%).

We evaluated two other camp models to further investigate and verify the above findings on the impact of timing of treatment on the cost-effectiveness of DAAs. The first treatment model was an alternate version of the *twice-treatment* model, wherein treatment was implemented at the beginning of the intervention period (year 0) and at the end of the 5th year, as opposed to at the end of the 5th and 10th years. The second treatment model was, similarly, an alternate version of the *thrice-treatment* model, with treatment at the end of the 0th, 3rd and 6th years, as opposed to at the end of the 3rd, 6th and 10th years. As done before, we computed the NMBs of these treatment models against that of the *annual-treatment* model for each value of uptake rate up to 90%, and found that both treatment models yielded negative values of the NMB at every uptake rate when compared to the *annual-treatment* model.

Therefore, the following key insight emerges from *RO2*: as uptake rates increase, within a

surveillance/intervention period that is significantly shorter (e.g., $< 50\%$) than the life expectancy of patients with the disease, it is evident that screening and treating less frequently appears beneficial. In particular, the importance of conducting a treatment camp at the end of the surveillance period is clearly emphasized by the above results.

We must emphasize here that while screening and treating less frequently (i.e., the *end-treatment* or the *twice-treatment* models) appears more cost-effective, doing so does yield significantly larger numbers of infections (see Figures 4b - 4d). Thus, if the goal is to eradicate HCV, then the default model remains the most effective with as high an uptake rate as possible.

Further, there are other effects of adopting treatment models that lead to larger numbers of HCV infections that may be worth considering prior to decision-making. For example, HCV infections are often accompanied by HIV co-infections, especially among injecting drug users. Similarly, given that the majority of infected IDUs are younger in age than the average Indian person, larger numbers of HCV infections mean more young people who are ineligible to donate blood or organs. If such ‘second order’ effects are unlikely to occur, then the *twice-treatment* or the *end-treatment* models appear to be the most cost-effective options - this is particularly the case if the diagnosis and treatment rate without camps is low.

5. Discussion

The first question that we attempt to answer in this study, via *ROI*, is: to what extent is the cost-effectiveness of DAAs underestimated if transmissions are not considered in a model designed for this purpose? The extent of penetration of treatment among those infected plays a key role in its epidemiological effectiveness and therefore its cost-effectiveness, and hence we answer this question by quantifying the extent of underestimation as a function of treatment uptake rate. We find that the extent of underestimation is considerable - exceeding 100% - at lower uptake rates than at higher uptake rates. Treatment uptake rates are low in India (WHO, 2024), with recent studies estimating it to be 21%, and hence our findings provide further evidence to support continued subsidization of HCV treatment with DAAs, especially in regions with prevalence comparable to that in the Punjab province (approximately 3%). These findings are likely applicable to other developing countries where prevalences are at a similar or higher level: for example, Pakistan, certain African countries and Uzbekistan, among others Lim et al. (2020); CDC (2024). From a modeling standpoint, this indicates that incorporating transmissions analyses situated in regions with high uptake may be less important than in regions with low uptake. Once again, this implies

that cost-effectiveness analyses studies conducted for DAAs in regions where uptake rates are low need to incorporate transmissions to accurately capture their health and economic value.

As part of *RO1*, we also provide a method to determine the extent to which the uptake of treatment must be increased by computing the *incremental NMB* associated with a given uptake rate. As mentioned before, while the question of determining the extent to which treatment uptake must be increased is controversial, our approach facilitates making this decision in resource-constrained health systems. This approach also aids decision-making around which population subgroups to prioritize for provision of subsidized treatment - for example, relatively less privileged groups may be prioritized. Once again, this approach may be more broadly applicable - for example, to the case of expanding treatment access for HIV/AIDS or tuberculosis.

The second set of questions that we attempt to answer through this study, as part of *RO2*, is around the timing and frequency of treatment within a disease surveillance period. The key insight that emerges from this analysis is that the speed at which the disease progresses in infected individuals as well as the speed with it spreads are vital to determining the optimal timing and frequency of organizing treatment drives in terms of overall economic benefit. For instance, for a slow-moving disease such as HCV, our analysis indicates that at least one treatment drive must be held at the end of the surveillance period to achieve maximum health and economic value. However, from an epidemiological standpoint - i.e., in terms of minimizing the number of infections, or eradication of the disease - treating only at the end of the surveillance period may not be effective.

A limitation of our analysis around *ROs* 1 and 2 involves the lack of longitudinal data to validate the trends in HCV epidemiology generated by the ABS. However, our medical collaborator with substantial clinical and public health experience in the treatment and surveillance of HCV in the state of Punjab provided face validation to the longitudinal outcomes generated by the model. Our analysis also did not incorporate indirect medical costs - such as those of the productivity losses of patients and their caregivers - due to limited availability of data. Addressing this limitation, and the conduct of a cost-effectiveness analysis of screening programs, provide avenues of future research. Another key avenue of future work, motivated by the findings from *RO2*, involves further investigation of the relationship between: (a) speed of infectious disease progression; (b) its spread, and (c) optimal frequency and timing of screening.

Our agent-based modeling analysis required the estimation of *lifetime horizon* health and economic outcomes to accomplish the above research objectives. Faced with limitations on the computational resources available for the analysis, we were motivated to develop our proposed *outcomes*

allocation approach for outcomes estimation that: (a) yielded *lifetime horizon* outcomes instead of settling for the less computationally intensive but also informationally incomplete *within-trial* approach, (b) preserved the stochasticity of outcomes afforded by simulation instead of assigning expected values of the outcomes to each infected agent, and (c) incurred substantially smaller computational expense.

The development of the OA approach for outcomes estimation motivates other avenues of research. For example, the current version of the approach still requires incremental accumulation of outcomes during the ABS execution horizon. It may be worth exploring whether repositories may be generated by stratifying across agent sample paths, where the number of possible sample paths is not too large, to obviate this requirement. This is likely to substantially further reduce the computational expense associated with such simulations. Similarly, exploring whether this approach can be extended to other types of dynamic infectious disease transmission models, such as compartmental models.

Overall, our study provides guidance for both policymakers and modelers, in terms of actionable insights regarding HCV, and more generally for slow-moving and relatively slow-spreading (in comparison to airborne pathogens) infectious diseases, such as HIV, where similar problems have been considered before in a deterministic setting, as in Deo et al. (2015). These include insights regarding screening and treatment program management for policymakers, and insights regarding when to incorporate transmissions and more efficient methods for outcomes estimation for modelers.

References

- Abualkhair, H., Lodree, E. J., & Davis, L. B. (2020). Managing volunteer convergence at disaster relief centers. *International Journal of Production Economics*, 220, 107399.
- Aggarwal, R., Chen, Q., Goel, A., Seguy, N., Pendse, R., Ayer, T., & Chhatwal, J. (2017). Cost-effectiveness of hepatitis C treatment using generic direct-acting antivirals available in India. *PloS one*, 12, e0176503.
- Ambekar, A., & Tripathi, B. (2008). *Size estimation of injecting drug use in Punjab and Haryana*. Technical Report UNAIDS.
- Ayer, T., Zhang, C., Bonifonte, A., Spaulding, A. C., & Chhatwal, J. (2019). Prioritizing hepatitis C treatment in US prisons. *Operations Research*, 67, 853–873.

- Ayoub, H., & Abu-Raddad, L. J. (2017). Impact of treatment on hepatitis C virus transmission and incidence in Egypt: A case for treatment as prevention. *Journal of Viral Hepatitis*, *24*, 486–495.
- Azim, T., Khan, S. I., Haseen, F., Huq, N. L., Henning, L., Pervez, M. M., Chowdhury, M. E., & Sarafian, I. (2008). HIV and AIDS in Bangladesh. *Journal of Health, Population, and Nutrition*, *26*, 311.
- Basu, A., & Maciejewski, M. L. (2019). Choosing a time horizon in cost and cost-effectiveness analyses. *JAMA*, *321*, 1096–1097.
- Bennett, H., Gordon, J., Jones, B., Ward, T., Webster, S., Kalsekar, A., Yuan, Y., Brenner, M., & McEwan, P. (2017). Hepatitis C disease transmission and treatment uptake: impact on the cost-effectiveness of new direct-acting antiviral therapies. *The European Journal of Health Economics*, *18*, 1001–1011.
- Bennett, H., McEwan, P., Sugrue, D., Kalsekar, A., & Yuan, Y. (2015). Assessing the long-term impact of treating hepatitis C virus (HCV)-infected people who inject drugs in the UK and the relationship between treatment uptake and efficacy on future infections. *PLoS One*, *10*, e0125846.
- Brennan, A., Chick, S. E., & Davies, R. (2006). A taxonomy of model structures for economic evaluation of health technologies. *Health Economics*, *15*, 1295–1310.
- CDC (2024). Hepatitis C: CDC yellow book.
<https://wwwnc.cdc.gov/travel/yellowbook/2024/infections-diseases/hepatitis-c>, accessed 12th July 2024.
- Chakravarti, A., Ashraf, A., & Malik, S. (2013). A study of changing trends of prevalence and genotypic distribution of hepatitis C virus among high risk groups in North India. *Indian Journal of Medical Microbiology*, *31*, 354–359.
- Chhatwal, J., He, T., & Lopez-Olivo, M. A. (2016). Systematic review of modelling approaches for the cost effectiveness of hepatitis C treatment with direct-acting antivirals. *Pharmacoeconomics*, *34*, 551–567.

- Chhatwal, J., Kanwal, F., Roberts, M. S., & Dunn, M. A. (2015). Cost-effectiveness and budget impact of hepatitis C virus treatment with sofosbuvir and ledipasvir in the United States. *Annals of internal medicine*, *162*, 397–406.
- Chugh, Y., Dhiman, R. K., Premkumar, M., Prinja, S., Singh Grover, G., & Bahuguna, P. (2019). Real-world cost-effectiveness of pan-genotypic sofosbuvir-velpatasvir combination versus genotype dependent directly acting anti-viral drugs for treatment of hepatitis C patients in the universal coverage scheme of Punjab state in India. *PLoS One*, *14*, e0221769.
- Chugh, Y., Premkumar, M., Grover, G. S., Dhiman, R. K., Teerawattananon, Y., & Prinja, S. (2021). Cost-effectiveness and budget impact analysis of facility-based screening and treatment of hepatitis C in Punjab state of India. *BMJ Open*, *11*, e042280.
- Cipriano, L. E., Zanic, G. S., Holodniy, M., Bendavid, E., Owens, D. K., & Brandeau, M. L. (2012). Cost effectiveness of screening strategies for early identification of HIV and HCV infection in injection drug users. *PloS One*, *7*, e45176.
- Cousien, A., Tran, V. C., Deuffic-Burban, S., Jauffret-Roustide, M., Dhersin, J.-S., & Yazdanpanah, Y. (2015). Dynamic modelling of hepatitis C virus transmission among people who inject drugs: a methodological review. *Journal of Viral Hepatitis*, *22*, 213–229.
- Cousien, A., Tran, V. C., Deuffic-Burban, S., Jauffret-Roustide, M., Dhersin, J.-S., & Yazdanpanah, Y. (2016). Hepatitis C treatment as prevention of viral transmission and liver-related morbidity in persons who inject drugs. *Hepatology*, *63*, 1090–1101.
- Cousien, A., Tran, V. C., Deuffic-Burban, S., Jauffret-Roustide, M., Mabileau, G., Dhersin, J.-S., & Yazdanpanah, Y. (2018). Effectiveness and cost-effectiveness of interventions targeting harm reduction and chronic hepatitis C cascade of care in people who inject drugs: the case of France. *Journal of Viral Hepatitis*, *25*, 1197–1207.
- Das, S., Ramamohan, V., & Mustafee, N. (2021). A discrete simulation optimization approach towards calibration of an agent-based simulation model of hepatitis C virus transmission. In *2021 Winter Simulation Conference (WSC)* (pp. 1–12). IEEE.
- Das, S., Sen, D., Ramamohan, V., & Sood, A. (2019). An agent-based model of hepatitis C virus transmission dynamics in India. In *Proceedings of the Winter Simulation Conference WSC '19* (p. 984–995). IEEE Press.

- Deo, M. G. (2013). Doctor population ratio for India-the reality. *The Indian Journal of Medical Research*, *137*, 632.
- Deo, S., Rajaram, K., Rath, S., Karmarkar, U. S., & Goetz, M. B. (2015). Planning for HIV screening, testing, and care at the veterans health administration. *Operations Research*, *63*, 287–304.
- Duijzer, L. E., van Jaarsveld, W., & Dekker, R. (2018). The benefits of combining early aspecific vaccination with later specific vaccination. *European Journal of Operational Research*, *271*, 606–619.
- Duma, D., & Aringhieri, R. (2023). Real-time resource allocation in the emergency department: A case study. *Omega*, *117*, 102844.
- Department of Economic & Social Affairs, U. N. (2019). World population prospects 2019. <https://population.un.org/wpp2019/Download/Standard/Mortality/>, accessed on 18th July, 2024.
- Epstein, R. L., Pramanick, T., Baptiste, D., Buzzee, B., Reese, P. P., Linas, B. P., & Sawinski, D. (2023). A microsimulation study of the cost-effectiveness of hepatitis C virus screening frequencies in hemodialysis centers. *The Journal of the American Society of Nephrology*, *34*, 205–219.
- Farhan, M., Fazal, F., Dave, T., Butt, A., Basit, J., & Maqbool, S. (2023). National hepatitis registry in Pakistan: a dire need for hepatitis surveillance and control. *Tropical Medicine and Health*, *51*, 41.
- Ghaderi, M. (2022). Public health interventions in the face of pandemics: Network structure, social distancing, and heterogeneity. *European Journal of Operational Research*, *298*, 1016–1031.
- Goel, A., Chen, Q., Chhatwal, J., & Aggarwal, R. (2018). Cost-effectiveness of generic pan-genotypic sofosbuvir/velpatasvir versus genotype-dependent direct-acting antivirals for hepatitis c treatment. *Journal of Gastroenterology and Hepatology*, *33*, 2029–2036.
- Gopalappa, C., Sansom, S. L., Farnham, P. G., & Chen, Y.-H. (2017). Combinations of interventions to achieve a national HIV incidence reduction goal: insights from an agent-based model. *AIDS*, *31*, 2533–2539.

- He, T., Li, K., Roberts, M. S., Spaulding, A. C., Ayer, T., Grefenstette, J. J., & Chhatwal, J. (2016). Prevention of hepatitis C by screening and treatment in US prisons. *Annals of Internal Medicine*, *164*, 84–92.
- Indiaspend (2017). Punjab: Slow growth, high unemployment big challenges for new government. <https://www.indiaspend.com/punjab-slow-growth-high-unemployment-big-challenges-for-new-government-39427/>, accessed 12th July 2024.
- IPEN Study Group et al. (2012). Injection practices in India. *WHO South-East Asia Journal of Public Health*, *1*, 189–200.
- Kim, S.-Y., & Goldie, S. J. (2008). Cost-effectiveness analyses of vaccination programmes: a focused review of modelling approaches. *Pharmacoeconomics*, *26*, 191–215.
- Kwon, J. A., Chambers, G. M., Luciani, F., Zhang, L., Kinathil, S., Kim, D., Thein, H.-H., Botha, W., Thompson, S., Lloyd, A. et al. (2021). Hepatitis C treatment strategies in prisons: A cost-effectiveness analysis. *Plos One*, *16*, e0245896.
- Lim, A. G., Walker, J. G., Mafirakureva, N., Khalid, G. G., Qureshi, H., Mahmood, H., Trickey, A., Fraser, H., Aslam, K., Falq, G. et al. (2020). Effects and cost of different strategies to eliminate hepatitis C virus transmission in Pakistan: a modelling analysis. *The Lancet Global Health*, *8*, e440–e450.
- Martin, N. K., Vickerman, P., Grebely, J., Hellard, M., Hutchinson, S. J., Lima, V. D., Foster, G. R., Dillon, J. F., Goldberg, D. J., Dore, G. J. et al. (2013). Hepatitis C virus treatment for prevention among people who inject drugs: modeling treatment scale-up in the age of direct-acting antivirals. *Hepatology*, *58*, 1598–1609.
- Micallef, J., Kaldor, J., & Dore, G. (2006). Spontaneous viral clearance following acute hepatitis c infection: a systematic review of longitudinal studies. *Journal of Viral Hepatitis*, *13*, 34–41.
- Ministry of Home Affairs, Government of India (2011). A-01: Number of villages, towns, households, population and area (India, states/uts, districts and sub-districts) - 2011, census of India 2011. <https://censusindia.gov.in/nada/index.php/catalog/42526>, accessed 12th July 2024.

Ministry of Statistics & Programme Implementation, Government of India (2023). First advance estimates of national income 2022-23. <https://www.mospi.gov.in/press-release/press-note-first-advance-estimates-national-income-2022-23>, accessed on 12th July 2024.

NACO (2018). National estimation of blood requirement in India. <https://naco.gov.in/sites/default/files/Final%20Estimation%20Report%20of%20Blood%20Requirement%20in%20India%20%281%29.pdf>, accessed 12th July 2024.

Nguyen, L. K. N., Howick, S., & Megiddo, I. (2024). A framework for conceptualising hybrid system dynamics and agent-based simulation models. *European Journal of Operational Research*, *315*, 1153–1166.

Olsen, J., & Jepsen, M. R. (2010). Human papillomavirus transmission and cost-effectiveness of introducing quadrivalent HPV vaccination in Denmark. *International Journal of Technology Assessment in Health Care*, *26*, 183–191.

Pala, A., Sorathiya, N., Noorani, N., Shah, J., Mehta, A., & Achnani, H. (2016). Assessment of sterilization at dental clinics in India- a cross-sectional study. *The Indian Journal of Medical Research*, *3(3)*, 31–33.

Prinja, S., Downey, L. E., Gauba, V. K., & Swaminathan, S. (2018). Health technology assessment for policy making in India: current scenario and way forward. *PharmacoEconomics-Open*, *2*, 1–3.

Rolls, D., Daraganova, G., Sacks-Davis, R., Hellard, M., Jenkinson, R., McBryde, E., Pattison, P., & Robins, G. (2012). Modelling hepatitis C transmission over a social network of injecting drug users. *Journal of Theoretical Biology*, *297*, 73–87.

van Santen, D. K., de Vos, A. S., Matser, A., Willemse, S. B., Lindenburg, K., Kretzschmar, M. E., Prins, M., & de Wit, G. A. (2016). Cost-effectiveness of hepatitis C treatment for people who inject drugs and the impact of the type of epidemic; extrapolating from Amsterdam, the Netherlands. *PLoS One*, *11*, e0163488.

Sargent, R. G. (2010). Verification and validation of simulation models. In *Proceedings of the 2010 winter simulation conference* (pp. 166–183). IEEE.

- Scott, N., McBryde, E. S., Thompson, A., Doyle, J. S., & Hellard, M. E. (2016). Treatment scale-up to achieve global HCV incidence and mortality elimination targets: a cost-effectiveness model. *Gut*, (pp. 1507–1515).
- Sood, A., Suryaprasad, A., Trickey, A., Kanchi, S., Midha, V., Foster, M., Bennett, E., Kamili, S., Alvarez-Bognar, F., Shadaker, S. et al. (2018). The burden of hepatitis C virus infection in Punjab, India: a population-based serosurvey. *PloS One*, *13*, e0200461.
- Statista (2018). Frequency of visiting or consulting with a dentist or dental surgeon in India as of May 2018. <https://www.statista.com/statistics/916681/india-frequency-of-dental-visits/>, accessed 12th July 2024.
- Weiser, T. G., Haynes, A. B., Molina, G., Lipsitz, S. R., Esquivel, M. M., Uribe-Leitz, T., Fu, R., Azad, T., Chao, T. E., Berry, W. R. et al. (2016). Size and distribution of the global volume of surgery in 2012. *Bulletin of the World Health Organization*, *94*, 201.
- WHO (2024). Global hepatitis report 2024: action for access in low- and middle-income countries. <https://www.who.int/publications/i/item/9789240091672>, accessed 12th July 2024.
- Willem, L. (2015). Agent-based models for infectious disease transmission. *Antwerp: University of Antwerp*, .

Appendix A. Hepatitis C Virus Infection Progression Module

Approximately 26% of those newly infected with HCV clear the infection within six months of being infected (Micallef et al., 2006). This is the acute state of HCV. Our clinical collaborator confirmed that the health and economic impacts of HCV were primarily associated with the chronic stages, and this is also supported in the literature (Chugh et al., 2019). The chronic states are divided into two groups - (i) early chronic states, and (ii) critical and advanced states. The early states include - in chronological order from first to last - the F0, F1, F2, F3 and F4 states wherein the liver is not damaged beyond cure. F4 is the first state of cirrhosis (compensated cirrhosis), and is followed by the first state in the second group - DC or decompensated cirrhosis. Following the DC state is HCC or hepatocellular carcinoma, which incurs substantial one-time as well as recurring management costs. Many patients in the DC and the HCC states have to undergo a liver transplant, and hence we incorporate this state as well in the DTMC. Finally, patients of states

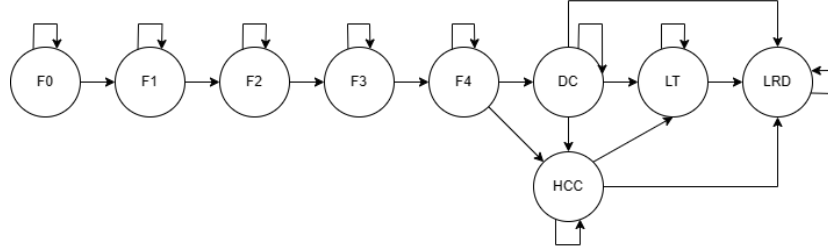


Figure A.5: The discrete-time Markov chain used to model the natural history of chronic HCV in an infected agent.

DC, HCC or even those who have had liver transplants can die of liver-related causes, and hence we incorporate an absorbing state for liver-related deaths (the LRD state). This DTMC is depicted in Figure A.5.

Infected agents can exit the fibrosis states (F0 - F3), the F4 and the DC states if they are cured - i.e., achieve sustained virologic response or SVR - via treatment with DAAs. Patients who achieve SVR from the cirrhotic states (DC or F4) may still experience transition to the DC or HCC states, albeit with a significantly reduced probability than if they still were infected, due to the damage their liver has already sustained.

The NH-DTMC is implemented as a Monte Carlo simulation for each individual infected agent to capture heterogeneity of outcomes possible with HCV. In other words, the progression of HCV for each infected agent can be considered as an *iid* replication of this simulation, conditional on the age of infection (or state of infection, if the agent is part of the initial cohort of infected agents).

The annual transition probabilities for the NH-DTMC (see Section 3) are given in Table A.7. The annual transition probability from DC to LRD (0.182) was higher in the first year than in the subsequent years (0.112). Similarly, the annual transition probability from LT to LRD was higher in the first year (0.116) than in the subsequent years (0.044). All the other transition probabilities remained constant over the sojourn of an agent in a particular state. We also incorporate the annual transition probabilities from the state SVR2 to states DC and HCC as discussed above in this section.

The implementation of the NH-DTMC and the non-DRM models as a Monte Carlo simulation replication for each infected agent is captured in Algorithm 4 below.

Table A.7: State transitions and transition probability estimates, for the natural history discrete-time Markov chain, obtained from Chhatwal et al. (2015).

Transition	Probability
Acute - Healthy	0.26 (Six months)
F0-F1; F1-F2; F2-F3; F3-F4	0.117; 0.085; 0.120; 0.116
F4-DC; F4-HCC	0.039; 0.014
DC-HCC; DC-LT; DC-LRD	0.068; 0.023; 0.182/0.112 (first year/after first year)
HCC-LT; HCC-LRD	0.040; 0.427
LT-LRD	0.116/0.044 (first year/after first year)
SVR2-DC; SVR2-HCC	0.008; 0.005

Algorithm 4 Infection status and health state update (execution of the NH-DTMC and non-DRD models) subroutine.

- 1: **Begin Initialization** ▷ Initialization phase
 - 2: Initialize with $K \times K$ transition probability matrix P for the NH-DTMC.
 - 3: Construct *cdf* for random variables X_k , where X_k represents the disease state in the next time point, for each $k \in \{1, 2, \dots, K\}$.
 - 4: **for** each $k \in \{1, 2, \dots, K\}$ **do**
 - 5: Identify the row of P corresponding to k .
 - 6: Identify non-zero entries of P .
 - 7: Construct *cdf* $F_k(x)$ corresponding to state k .
 - 8: Example: for disease state k , k -th row of P is identified.
 - 9: Let non-zero entries be $p_{k1}, p_{k2}, \dots, p_{kK}$ ($k \leq K$).
 - 10: Step points for *cdf* $F_k(x)$: $p_{k1}, p_{k1} + p_{k2}, p_{k1} + p_{k2} + p_{k3}$ and so on.
 - 11: **end for**
 - 12: **End Initialization** ▷ End of initialization phase
 - 13: Current infection status of agent $Inf_t := 1$.
 - 14: Current disease state of agent $k_t := k$.
 - 15: **while** agent is alive AND $Inf_t = 1$ **do**
 - 16: Execute non-DRM model: if agent is alive, proceed; else, BREAK.
 - 17: Is patient cured? If yes, $Inf_t = 0$, BREAK; else $Inf_t = 1$, proceed.
 - 18: Identify *cdf* $F_k(x)$ corresponding to k .
 - 19: Sample $u = U(0, 1)$.
 - 20: Set new state as $k_t = F_k^{-1}(u)$.
 - 21: **end while**
-

Appendix B. Treatment Module of the Agent-based Simulation Model: Additional Details

In Table B.8, we provide an example of the implementation of the *annual-treatment* algorithm (described in Section 3.2). Untreated infections in every time period are treated according to its corresponding coverage rate. For example, of 20 infections caused at time point 1, 14 are assigned to treatment. At $j = 1$, 52% of these 14 infections are treated. Of the remaining infections among these, 64% are treated at time point 2. Bold-faced numbers indicate that the total number of new infections *and* treatment assignments in each time period matches the respective number of treatment assignments.

Table B.8: Example illustrating the implementation of the *annual-treatment* algorithm. $u = 0.7, \alpha = 0.4$, and $n = 5$.

Time period	Number of new infections	Number of new infections assigned to treatment	Coverage fraction for treatment-assigned patients	Number of infections treated among those caused at time point					
				0	1	2	3	4	5
0	100	70	0.40	28.00	-	-	-	-	-
1	20	14	0.52	21.84	7.28	-	-	-	-
2	16	11.2	0.64	12.90	4.30	7.17	-	-	-
3	12	8.4	0.76	5.52	1.84	3.06	6.384	-	-
4	8	5.6	0.88	1.53	0.51	0.85	1.774	4.93	-
5	4	2.8	1.00	0.21	0.07	0.12	0.242	0.67	2.80
Total	160	112	--	70	14	11.2	8.4	5.6	2.8

We now provide a straightforward mathematical argument to show that Algorithm 1 yields the required treatment uptake rate under deterministic conditions. For this, it is sufficient to show that among infections caused at any time point j_1 , $0 \leq j_1 \leq n$, the number of these infections undergoing treatment will be equal to the number of these infections assigned to treatment. In other words, we need to show:

$$\sum_{j=j_1}^n N_{j_1,j}^{Tr} = N_{j_1}^a, \quad j_1 = 0, 1, \dots, n \quad (\text{B.1})$$

We first note that the coverage fraction for treatment-assigned patients for time period j_1 is $[\alpha + \{(1 - \alpha) \times \frac{j_1}{n}\}]$, the number of infections created and assigned to treatment that are also treated at j_1 is given by:

$$N_{j_1,j_1}^{Tr} = [\alpha + \{(1 - \alpha) \times \frac{j_1}{n}\}] \times N_{j_1}^a \quad (\text{B.2})$$

Consider an agent that acquires an infection at j_1 . Assume that the event that it does not get treated at j_2 , where $0 \leq j_1 < j_2 \leq n$, is independent of the event that it has been untreated till time point $(j_2 - 1)$. The probability that any treatment-assigned infection created at time point j_1 gets treated at a time point j , where $0 \leq j_1 < j < n$ is the coverage fraction $[\alpha + \{(1 - \alpha) \times \frac{j_1}{n}\}]$.

Hence, the probability that any treatment-assigned infection (created at time point j_1) does not get treated at time point j , where $0 \leq j_1 < j \leq n$ is given by the expression:

$$1 - [\alpha + \{(1 - \alpha) \times \frac{j}{n}\}] = [(1 - \alpha) - \{(1 - \alpha) \times \frac{j}{n}\}]$$

Thus, the probability of any treatment-assigned infection (created at time point j_1) not being treated till time point $(j_2 - 1)$, where $0 \leq j_1 < (j_2 - 1) \leq n$, is given by the expression:

$$\prod_{j=j_1}^{j_2-1} [(1 - \alpha) - \{(1 - \alpha) \times \frac{j}{n}\}]$$

Moreover, we assume that the event of the agent being treated at time point j_2 is independent of the event that it has not been treated until the time point $(j_2 - 1)$. Then the probability of the agent not being treated until time point $(j_2 - 1)$ and then being treated at j_2 is given by:

$$\prod_{j=j_1}^{(j_2-1)} [(1 - \alpha) - \{(1 - \alpha) \times \frac{j}{n}\}] \times [\alpha + \{(1 - \alpha) \times \frac{j_2}{n}\}] \quad (\text{B.3})$$

Thus, the number of infections caused at time point j_1 and treated at time point j_2 is given by:

$$\begin{aligned} N_{j_1, j_2}^{Tr} &= \prod_{j=j_1}^{j_2-1} [(1 - \alpha) - \{(1 - \alpha) \times \frac{j}{n}\}] \times [\alpha + \{(1 - \alpha) \times \frac{j_2}{n}\}] \times N_{j_1}^a, \quad 0 \\ &\leq j_1 < (j_2 - 1) \leq n \end{aligned}$$

If $j_2 = n$, then the above equation becomes:

$$N_{j_1, n}^{Tr} = \prod_{j=j_1}^{n-1} [(1 - \alpha) - \{(1 - \alpha) \times \frac{j}{n}\}] \times [\alpha + \{(1 - \alpha) \times \frac{n}{n}\}] \times N_{j_1}^a, \quad 0 \leq j_1 < n \quad (\text{B.4})$$

Note: for the case $j_1 = n$, $N_{n, n}^{Tr} = N_n^a$ and we are done.

Now, equation B.4 can be written as:

$$\begin{aligned}
N_{j_1, n}^{Tr} &= \prod_{j=j_1}^{n-1} \left[(1-\alpha) - \left((1-\alpha) \times \frac{j}{n} \right) \right] \times N_{j_1}^a, \quad 0 \leq j_1 < n \\
&= \prod_{j=j_1}^{n-2} \left[(1-\alpha) - \left((1-\alpha) \times \frac{j}{n} \right) \right] \\
&\quad \times \left[(1-\alpha) - \left((1-\alpha) \times \frac{n-1}{n} \right) \right] \times N_{j_1}^a, \quad 0 \leq j_1 < n
\end{aligned} \tag{B.5}$$

Then, we have:

$$\begin{aligned}
N_{j_1, (n-1)}^{Tr} &= \prod_{j=j_1}^{n-2} [(1-\alpha) - \{(1-\alpha) \times \frac{j}{n}\}] \\
&\quad \times [\alpha + \{(1-\alpha) \times \frac{n-1}{n}\}] \times N_{j_1}^a, \quad 0 \leq j_1 < (n-1)
\end{aligned} \tag{B.6}$$

Adding equations B.5 and B.6, we get:

$$\begin{aligned}
N_{j_1, n}^{Tr} + N_{j_1, (n-1)}^{Tr} &= \prod_{j=j_1}^{n-2} [(1-\alpha) - \{(1-\alpha) \times \frac{j}{n}\}] \\
&\quad \times N_{j_1}^a, \quad 0 \leq j_1 < (n-1) \\
&= \prod_{j=j_1}^{n-3} [(1-\alpha) - \{(1-\alpha) \times \frac{j}{n}\}] \\
&\quad \times [(1-\alpha) - \{(1-\alpha) \times \frac{n-2}{n}\}] \times N_{j_1}^a, \quad 0 \leq j_1 < (n-1)
\end{aligned} \tag{B.7}$$

Also:

$$\begin{aligned}
N_{j_1, (n-2)}^{Tr} &= \prod_{j=j_1}^{n-3} [(1-\alpha) - \{(1-\alpha) \times \frac{j}{n}\}] \\
&\quad \times [\alpha + \{(1-\alpha) \times \frac{n-2}{n}\}] \times N_{j_1}^a, \quad 0 \leq j_1 < (n-2)
\end{aligned} \tag{B.8}$$

Adding equations B.7 and B.8, we get:

$$\begin{aligned}
N_{j_1, n}^{Tr} + N_{j_1, (n-1)}^{Tr} + N_{j_1, (n-2)}^{Tr} &= \prod_{j=j_1}^{n-3} [(1-\alpha) - \{(1-\alpha) \times \frac{j}{n}\}] \\
&\quad \times N_{j_1}^a, \quad 0 \leq j_1 < (n-2)
\end{aligned} \tag{B.9}$$

Proceeding similarly as above, we get:

$$\sum_{j=j_1+1}^n N_j^{Tr} = [(1 - \alpha) - \{(1 - \alpha) \times \frac{j_1}{n}\}] \times N_{j_1}^a \quad (\text{B.10})$$

Adding equations B.2 and B.10, we get:

$$\sum_{j=j_1}^n N_j^{Tr} = N_{j_1}^a$$

Appendix C. Model Calibration, Verification and Validation

The verification and validation exercise for this model involves examining each of its modules for internal and external validity. We describe this process in this section.

First, we consider the agent-based transmission dynamics component of the model. Validating this component would ideally involve comparing the key disease transmission outcomes across time generated by the model - the extent of the spread of the disease - against external longitudinal data. The relevant disease transmission outcomes in our case are: (a) the HCV antibody prevalence, which is the proportion of the population (agent cohort) who have ever been infected with HCV, including active and previous (cured) infections; (b) the HCV RNA prevalence, the proportion of the population with active HCV infections; and (c) the IDU prevalence, the proportion of the population actively engaging in injecting drug use. In the Indian context, to the best of our knowledge, longitudinal data for the spread of HCV in Punjab is not available; however, reliable cross-sectional data is available. Therefore, for validating this component, we compare the HCV antibody, RNA and the IDU prevalence estimates generated by the model at a suitably chosen time point with corresponding estimates from the relevant epidemiological literature. We chose the study by Sood et al. (2018) for estimates of these outcomes, as it is possibly the largest cross-sectional study of the burden of HCV conducted for the state of Punjab. The study reported an HCV antibody prevalence of 3.6% (95% CI: 3.0 - 4.2%), an HCV RNA prevalence of 2.6% (2.0 - 3.1%) and an IDU prevalence of 0.1% (95% CI not reported).

At this stage, we recall that estimates of all input parameters for the transmission module were not available, and three parameters were designated as ‘calibration variables’ to be estimated via the model calibration process. The calibration process involved running the simulation model for a period of 50 years and varying the values of these parameters systematically until the key transmission-related or epidemiological outcomes (the HCV antibody, RNA and IDU prevalences)

of the model were suitably close to those mentioned above (henceforth referred to as calibration targets). Thus the validation process for these epidemiological model outcomes becomes the ‘calibration’ process.

There is more than one way to conduct the calibration process. For example, in a previous version of this model, the authors cast the calibration process for estimating the calibration variables as a discrete simulation optimization problem (Das et al., 2021). Guided by the calibration variable estimates obtained by Das et al. (2021), we obtained estimates of the calibration variables via a manual search. Our stopping criterion was as follows. We conduct 30 replications of the simulation until the end of the calibration period (50 years) for a given set of values of the calibration variables. At the end of the calibration period, we calculate the average value of each epidemiological outcome, denoted by: \hat{o}_1 = average HCV antibody prevalence, \hat{o}_2 = average HCV RNA prevalence, and \hat{o}_3 = average IDU prevalence (here $\hat{o}_i = \frac{1}{n} \sum_{j=1}^{30} \hat{o}_{ij}$). We then define the absolute value of the relative fractional deviation of each \hat{o}_i ($i \in \{1, 2, 3\}$) from its calibration target o_i ($i \in \{1, 2, 3\}$) as $d_i = \frac{|o_i - \hat{o}_i|}{o_i}$, $i \in \{1, 2, 3\}$. If the sum of the d_i ($i \in \{1, 2, 3\}$) is less than 0.2, indicating an average absolute fractional error of less than 7% across the epidemiological outcomes, we terminate the calibration process.

From the calibration process, the probability of acquiring an HCV infection from a contaminated medical environment, the probability of a non-IDU being converted to an IDU, and probability of IDUs engaging in needle-sharing during a group injecting event were estimated as 0.004, 2.8×10^{-5} and 0.41, respectively. From the estimate of probability of acquiring an HCV infection from a contaminated medical environment, the probability of HCV transmission via a contaminated blood transfusion was estimated as 0.806 using equation 3 in section 3.1.1. Based on the clinical literature (Chakravarti et al., 2013), it is evident that not every contaminated blood transfusion results in HCV transmission, and hence this estimate appears reasonable.

Model estimates of the key epidemiological outcomes at the end of the calibration period are provided in Table C.9. We observe coefficients of variation of approximately 20%, indicating relatively stable model performance. It is evident from the table that there is no statistically significant difference (at a 5% level of significance) between the model estimates of the epidemiological outcomes and the calibration targets.

An additional level of validation for the disease transmission component of the agent-based model, distinct from the calibration process, was carried out by comparing estimates of the contribution of the medical and social interaction environments to corresponding real-world observations

Table C.9: Key epidemiological outcomes obtained from the model calibration process. SD = standard deviation.

Epidemiological outcome	Calibration target (95% CI)	Model outcome: mean (SD)
HCV antibody prevalence	3.60% (3.0 - 4.2%)	3.57% (0.75%)
HCV RNA prevalence	2.60% (2.0 - 3.1%)	2.77% (0.58%)
IDU prevalence	0.10% (not reported)	0.10% (0.01%)

in the Indian context reported by Chakravarti et al. (2013). The authors reported on the prevalence of HCV infections among a cohort in a North Indian state located close to Punjab. The authors reported that 74.1% of the HCV infections they studied were caused due to unsafe medical procedures, 16.7% due to injecting drug use and 9% with tattooing. Given that infections due to tattooing were subsumed within the social interaction environment in our model, we compared the model estimates of the contributions of each environment to the total number of HCV infections across the calibration period to the corresponding contributions from the study by Chakravarti et al. (2013). The proportion of HCV infections caused in the medical environment was estimated (from 30 replications) as 73.6% with a standard deviation of 2.9%. A one-sample t -test for equality of means did not find this difference (compared to 74.1%) to be statistically significant at a significance level of 0.05. The contribution of the social interaction environment was estimated as 26.4% (standard deviation of 2.9%), against the value of 25.7% (sum of the contributions of injecting drug use and tattooing) reported in Chakravarti et al. (2013). Once again, this difference was not found to be statistically significant via a similar t -test.

The disease progression and non-DRD components of the simulation were validated by comparing outcomes from our models to outcomes from two studies conducted in the Indian context - Aggarwal et al. (2017) and Chugh et al. (2019) - after using initial conditions similar to those used in these studies.

Aggarwal et al. (2017) evaluated the cost-effectiveness of HCV treatment with DAAs using a DTMC for modeling disease progression among a cohort of patients aged 35 years (transmission dynamics were not considered). They estimated the average life years lived by chronic non-cirrhotic patients (states $F0 - F3$) to be 30.25 years, bringing the average life expectancy of these patients to 65.25 years. We used the HCV stage-wise initial distribution of patients from Aggarwal et al. (2017); however, we used the age-wise population distribution of Punjab in the year 2011 (Ministry of Home Affairs, Government of India, 2011), when the last census was carried out, yielding a median agent age of 29 years. Under these conditions, our model estimated the average life years lived by patients from states $F0 - F3$ to be 35.3 years, yielding an average life expectancy of 64.3

years for patients in HCV stages $F0–F3$. This is comparable to the estimate obtained by Aggarwal et al. (2017).

We also considered the study of Chugh et al. (2019) who perform a similar cost-effectiveness analysis with a different set of DAAs. The authors state that the average life expectancy of non-cirrhotic chronic patients is similar to that of the average life expectancy in the general population. Using the age-wise population distribution of Chugh et al. (2019) in our model, we estimated the average life years lived by non-cirrhotic chronic patients to be 38.3 years. This yielded an average life expectancy of 67.3 years, which corresponded to the reported life expectancy of India of 68.5 years in 2015 (Department of Economic & Social Affairs, 2019).

Several other internal and external verification and validation checks were performed, in line with recommendations by Sargent (2010) for simulation models. These included extreme condition tests for key input parameters, validation of the demographic module, and validation of key model inputs and outputs by our expert clinical collaborator.

Appendix D. Outcomes Estimation: Additional Details

The unit costs and resource use associated with HCV management are provided in Table D.11. The utility weights capturing the age-related deterioration in quality of life by age group and HCV disease state are provided in Table D.10.

Table D.10: Utility weights or quality-of life multipliers according to disease state and age group. The disease state utility weights were obtained from Chugh et al. (2019) and the age-based utility weights from He et al. (2016).

	HCV disease state	Utility weight		Age group (in years)	Utility weight
	Disease state utility weight	F0-F3		0.63	Age-based utility weight
F4		0.56	30-39	0.906	
DC		0.44	40-49	0.875	
HCC		0.44	50-59	0.849	
LT		0.84	60-69	0.826	
SVR2		0.93	70-79	0.786	
Healthy		1	80+	0.753	

Table D.11: Unit costs and resource use for HCV management. All costs are in INR.

F0-F3	F4	DC	HCC	LT
One-time cost heads and values				
CBC, 200	CBC, 200	CBC, 200	Surgery, 150000	Transplant, 2000000
LFT, 500	RBS, 100	RBS, 100	RFA (30% of patients), 150000	Others, 500000
RBS, 100	KFT, 300	TSH, 200	TACE (30% of patients), 150000	
KFT, 300	TSH, 200	HbsAg, 300	MWA (30% of patients), 150000	
TSH, 200	HbsAg, 300	Anti-HIV, 300	Radiation (5% of patients), 100000	
HbsAg, 300	Anti-HIV, 300	Fibroscan, 1500	TARE (1% of patients), 750000	
Anti-HIV, 300	Fibroscan, 1500		Costs from heads in DC state, 2600	
USG 500				
Fibroscan, 1500				
Net: 3900	Net: 2900	Net: 2600	Net: 300100	Net: 2500000
Recurring cost heads, annual frequency and values				
Doctor visits, 6, 500	Doctor visits, 6, 500	Doctor visits, 6, 500	Drugs (30% of patients), 50000	Drugs and others, 24000
PPIs, 8 courses, 1000	PPIs, 8 courses, 1000	PPIs, 8 courses, 1000	BSC (40% of patients), 12, 2500	
	USG, 2, 500	USG, 2, 500	Costs from heads in DC state, 23600	
	LFT, 2, 500	LFT, 2, 500		
	Hospitalization (10% of patients), 2, 25000	KFT, 4, 100		
	Endoscopy, 1, 3000	Hospitalization (10% of patients), 2, 25000		
	AFP, 1, 700	Endoscopy, 1, 3000		
		PTI, 4, 100		
Net: 11000	Net: 21700	Net: 23600	Net: 50600	Net: 24000

Notes. INR: Indian Rupee, CBC: complete blood count, LFT: liver function test, RBS: random blood sugar, KFT: kidney function test, TSH: thyroid stimulating hormone, HbsAg: surface antigen of hepatitis B virus (HBV), anti-HIV: HIV antibody test, USG: ultrasonography, RFA: radiofrequency ablation, TACE: transarterial chemoembolization, MWA: microwave ablation, TARE: background transarterial chemoembolization, PPIs: proton pump inhibitors, AFP: alpha-fetoprotein, PTI: prothrombin-time, BSC: best supportive care.